BOREAS An international journal of Quaternary research

Untangling nutrient co-regulation of ombrotrophic peatland development

RICHARD C. CHIVERRELL, DANIEL N. SCHILLEREFF, FIONA E. RUSSELL, JULIE VALENTINE, JASON R. KIRBY, DAVID M. WILKINSON AND JOHN F. BOYLE

BOREAS

Chiverrell, R. C., Schillereff, D. N., Russell, F. E., Valentine, J., Kirby, J. R., Wilkinson, D. M. & Boyle, J. F.: Untangling nutrient co-regulation of ombrotrophic peatland development. *Boreas*. https://doi.org/10.1111/bor.70031. ISSN 0300-9483.

Ombrotrophic peatlands are the largest terrestrial store of global carbon (C). While hydroclimate controls over peatland development are well known, the importance of nutrient fluxes has been researched less. Atmospheric nutrient fluxes to peatlands have increased with human activity in recent centuries. Here we explore the interplay of nutrient and hydroclimate drivers at Holcroft Moss (northwest England), a lowland ombrotrophic peatland typical of many across northern Europe. Parallel multi-proxy characterization of the organic matter composition and nutrient accumulation rates shows a sequence dominated by switches between fresh less decomposed layers and more decomposed peat containing abundant recalcitrant organic compounds. Hydroclimate variability governs much of the stratigraphy. Shifts to wetter conditions appear to trigger periods of reduced decomposition centred *c*. 3450, 2600–2500, 2225, 2060, 2000, 1825, 1650–1610, 1540, 1480, 1260, 1125, 1000, 740–720 and 600–550 cal. a BP. In addition, elevated N and P deposition beginning ~1000 cal. a BP, accelerating ~500 years cal. a BP, has led to changes in the co-behaviour between hydroclimate, peat composition and C accumulation rates. Long-term carbon/nutrient accumulation rates at Holcroft Moss are high compared to other UK peatlands measured to date. Higher nutrient fluxes from human activities will persist through the 21st century, with the implications for long-term peatland resilience and this important carbon sink unclear. Restoration and management of peatlands understandably focus on hydrology and vegetation, but we show a parallel need to consider nutrient deposition, which will vary site by site.

Richard C. Chiverrell (rchiv@liverpool.ac.uk), Fiona E. Russell and John F. Boyle, Department of Geography and Planning, University of Liverpool, Roxby Building, Liverpool L69 7ZT, UK; Daniel N. Schillereff, Department of Geography, King's College London, Bush House North East Wing, 30 Aldwych, WC2B 4BG London, UK; Julie Valentine and Jason R. Kirby, School of Biological and Environmental Science, Liverpool John Moores University, Byrom Street, Liverpool, Merseyside L3 3AF, UK; David M. Wilkinson, School of Natural Sciences, University of Lincoln, Brayford Pool, Lincoln LN6 7TS, UK; *received 7th March 2025, accepted 24th July 2025.*

Carbon (C) sequestration is a fundamental ecological process and important in the context of global change (Wilkinson 2023). Northern extratropical peatlands form the largest surface terrestrial store of global carbon and comprise approximately 500 Pg of the global soil carbon pool (Yu *et al*. 2010; Loisel *et al*. 2014, 2017). Ombrotrophic peatlands are regulated heavily by changing surface wetness (Barber 1981; Clymo 1983, 1984b; Gore 1983; Charman 2002; Barber & Charman 2014) and so are coupled to the balance between precipitation inputs and evapotranspiration losses. This coupling means that peat stratigraphy often preserves signals of past hydroclimate (Charman *et al*. 2004, 2006, 2013), although not always, given how autogenic peatland processes can respond to climate (Swindles *et al*. 2012). Given their nutrient-limited status, human-amplified nutrient deposition also impacts on the biogeochemical cycling of peatlands globally and affects carbon storage (Aerts *et al*. 1992; Toberman *et al*. 2015; Schillereff *et al*. 2021). These impacts include variations in primary productivity, decomposition and changes in peatland vegetation. The replacement of mosses (e.g. *Sphagnum*) by grasses and shrubs that have higher nutrient demands is becoming a common observation (McClymont *et al*. 2009; Swindles *et al*. 2015). These changes are happening in concert with changes in moisture regimes and climate warming (Mauquoy & Barber 1999a; Swindles *et al*. 2015), but also conversely, have included transitions from meso-oligotrophic fens to bogs with an expansion of *Sphagnum* (Magnan *et al*. 2018).

Research to untangle these hydroclimatic and nutrient drivers has largely involved fertilization experiments. Shifts in vegetation composition, microbial activity and rates of carbon sequestration have all been observed in response to N and P fertilization, admittedly against a backdrop of already elevated nutrient deposition (Limpens *et al*. 2004, 2006; Fritz *et al*. 2012; Lin *et al*. 2014). This type of experimental work, however, does not represent the full range of historical nutrient deposition rates, and results seem to show year-on-year transience in experiments that monitor on a timescale of days to a maximum of a couple of decades (Vitousek *et al*. 1997; Holland *et al*. 1999; Legrand *et al*. 2023). It is less clear how these results capture the decadal to millennial botanical and biogeochemical dynamics of peatland evolution. Peat stratigraphical studies have investigated how vegetation composition, organic matter characteristics and decomposition co-vary, but most consider only one or two components (e.g. effects of N or P on C accumulation) (Schillereff *et al*. 2021; Yang *et al*. 2023). Schillereff *et al*. (2021) using a database of P≡N≡C stoichiometry compiled for deep mid-latitude ombrotrophic peatlands, found that long-term elevated P deposition and accumulation correlated

DOI 10.1111/bor.70031

strongly with increased organic matter decomposition and lower C accumulation. Though based on relatively few sites globally (n = 12) (Schillereff *et al.* 2021), those long-term patterns contrast with studies that show short-term increases in P supply stimulate C accumulation (Limpens *et al.* 2006; Fritz *et al.* 2012).

Palaeoenvironmental records have been accessed from peatlands for more than a century (Blytt 1876; Weber 1903; Sernander 1908; von Post 1909; Granlund 1932). Ombrotrophic peatlands grow, accumulate mass and sequester C when the production of vegetation outpaces the decay of organic matter. Living plants take up C through photosynthesis from atmospheric carbon dioxide (CO_2) for the most part, with an additional contribution via the fixation of 'old' CO_2 from soil respiration (Kilian *et al.* 1995; Chambers *et al.* 2011). C is lost from peatlands via decay processes both as gaseous loss (CO_2, CH_4) to the atmosphere and aqueous loss from drainage to watercourses. Most of the vegetation decay takes place aerobically in the surface layers of peat above the water table. The aerobic breakdown and decomposition of plant matter into organic compounds (e.g. humic acid) is termed 'humification', but decay continues also under anaerobic conditions at a much slower rate by microbial digestion and release of primary minerals and CO_2/CH_4. Techniques used traditionally to measure the state of decay or humification of peat are based on either quantifying the degradation of plant remains or the accumulated decay products, and increasingly use more complex genomic, spectroscopic and calorific methods in their quantification (Biester *et al.* 2014; Zaccone *et al.* 2018).

Peatland development research often addresses one or two factors, even though the effects on carbon sequestration are typically multifaceted and compound or interactive (e.g. hydroclimate, N, P, etc) (Tipping *et al.* 2017; Schillereff *et al.* 2021). Here we explore how hydroclimatic and nutrient factors interact using high-resolution proxy data reconstructing long-term changes in peatland development spanning ~4300 years from a radiocarbon dated sequence at Holcroft Moss (northwest England). New and previously published (Birks 1965; Garcés-Pastor *et al.* 2023) pollen investigations for Holcroft Moss provide information on changing regional land cover. Plant macrofossil and subfossil testate amoebae records for Holcroft Moss provide information on peatland vegetation and long-term changing water tables (e.g. Charman *et al.* 1999, 2006; Amesbury *et al.* 2016). Multi-method characterization of the organic matter stratigraphy was conducted quantifying the organic components and functional groups by Fourier transform Infrared (FTIR), Fourier transform near-infrared (FT-NIR) spectroscopy, thermogravimetric analysis (TGA) and measuring the concentrations of total humic compounds (e.g. alkali extraction methods). Geochemical methods were used to determine nutrient (e.g. C, N, P, K, Ca) concentrations and accumulation rates. The aim is to assess the interplay of nutrient and hydroclimate drivers on peatland development for a lowland ombrotrophic system typical of many across NW Europe.

Site background and methods

Study site, fieldwork and subsampling

Holcroft Moss is part of a swath of lowland ombrotrophic bogs west and north of Manchester (Fig. 1) (Birks 1965; Leah *et al.* 1997; Valentine *et al.* 2013; Fletcher & Ryan 2018; Garcés-Pastor *et al.* 2023). Chat Moss, the largest expanse of peat, occupied formerly an area >42 km^2, with Holcroft Moss >2.25 km^2 and Risley Moss further west >7 km^2 (Leah *et al.* 1997). These peatlands have been heavily denuded by drainage, conversion to agricultural lands and commercial peat extraction. As a Site of Special Scientific Interest (SSSI) and National Nature Reserve (NNR), Holcroft Moss is the only intact remnant of the former central dome and the only area of uncut lowland bog in Cheshire (Birks 1965; Leah *et al.* 1997). Restoration work has been undertaken at Holcroft Moss by Cheshire Wildlife Trust, designed to maintain water retention on the bog (Valentine *et al.* 2013). Purple moor grass (*Molinia caerulae*) is presently the dominant vegetation, but restoration efforts have increased the abundance of *Erica tetralix*, *Vaccinium*, *Eriophorum* and *Sphagnum* species. In 2012, two bisecting transects of cores confirmed a consistent stratigraphical sequence that was relatively unchanged from Birks (1965). Three parallel duplicate master core profiles were recovered from the centre of the site (53.4354°N, 2.4753°W) with analysis focused on a single master profile (Fig. 1). Water contents were estimated using the ratio of coherent to incoherent X-ray scattering data obtained during wet whole-core scanning at 5 mm intervals on a GEOTEK/Olympus DELTA μXRF Multi-Sensor Core Logger (Geotek-MSCL) (Boyle *et al.* 2015). Down-core profiles for water content (%) were used to calculate peat dry mass accumulation rates checked against spot measurements of volumetric wet and dry mass.

Geochronology

Age control for the peat sequence was secured by 13 Accelerator Mass Spectrometer (AMS) ^{14}C measurements supported by the use of near surface airborne pollution markers dated independently within the region. These included atmospheric airfall Pb (Le Roux *et al.* 2004; Goldsmith *et al.* 2013), Spheroidal Carbonaceous Particles (SCPs) (Rose & Appleby 2005; Garcés-Pastor *et al.* 2023), and mineral dusts (Ti and Zr) linked to adjacent motorway construction and opening. The ^{14}C measurements were all obtained for handpicked plant macrofossils, mostly *Sphagnum* remains, to negate

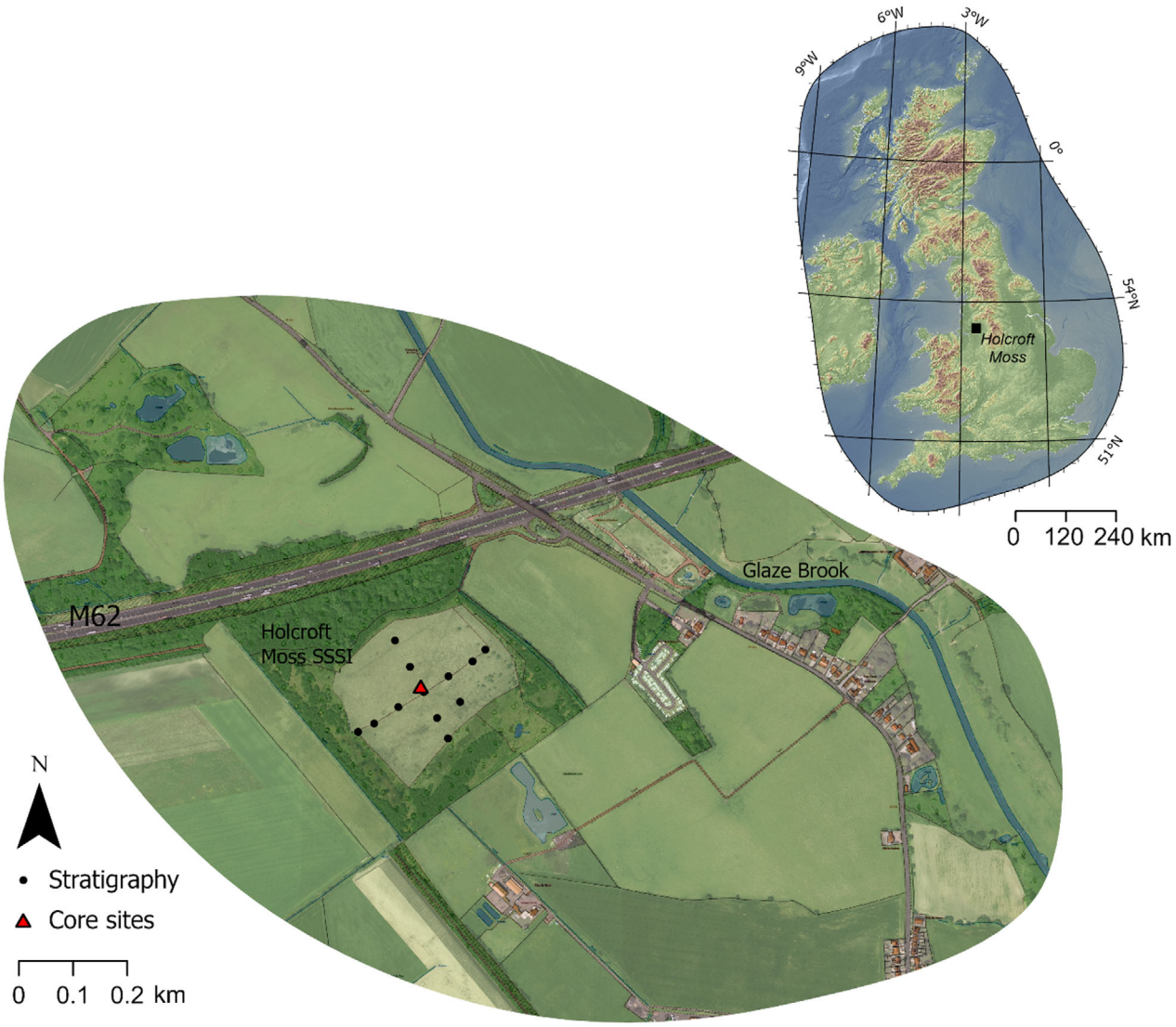

Fig. 1. Holcroft Moss (NW England) showing the core transects and the triangle (53.4354°N, 2.4753°W) denoting the location of the three duplicate cores (HM2012). Aerial imagery © Getmapping PLC and contains OS data © Crown copyright (2020).

issues associated with the dating of peat bulk or organic fractions (Kilian *et al.* 1995) and downward penetration of vascular plant roots (Table 1). ^{14}C measurements were conducted at both the Scottish Universities Environmental Research Centre (SUERC) and Beta Analytic (Beta) radiocarbon laboratories.

Palaeoecology

The palaeoecology analyses focused on quantifying the amoebic protists (testate amoebae), macrofossil plant remains and subfossil pollen. Pollen preparations followed standard procedures (Moore *et al.* 1991), with identification and counting at 400× using a Zeiss Axiovision phase contrast light microscope with reference to Moore *et al.* (1991) and the Liverpool John Moores University pollen reference collection. All pollen/spore counts were converted to percentages of land pollen and plotted using TGview software (Grimm 1991) (Fig. S1). Plant macrofossil analyses followed a modified quadrate and leaf count procedure (Mauquoy & Barber 1999b; Chiverrell 2001) that involved quantification of the major macrofossil components under low power microscopy using a randomized 10 × 10 mm grid in petri dishes. Decile scores (1–10) were given to each component per 100 mm^2 squares, except for macroscopic charcoal fragments which were counted. The major components: total *Sphagnum*, Monocotyledon, Ericaceous, other Bryophytes and Unidentifiable Organic Matter (UOM) remains were totalled and converted to percentages. To subdivide the *Sphagnum* into species, 100 leaves were identified and counted under a microscope (×400)

Table 1. Accelerator mass spectrometer ^{14}C measurements and pollutant age-depth chronological markers.

Sample ID/Lab. code	Age (a BP)	Error (a)	Depth (cm)	Chronological materials	Median (cal. a BP)	1 sigma range (cal. a BP) (min.)	1 sigma range (cal. a BP) (max.)
Top of profile	−62	1	0	Top of core = sample date	−62	−63	−61
SCP-peak	−27	5	8	Peak in SCPs (Fig. 2A)	−28	−34	−23
M62 built	−10	5	15	Dust deposition (Fig. 2A)	−6	−12	−0
SCP rise	0	10	15	SCP rise (Fig. 2A)	−6	−12	−0
Pb-rise	50	15	26	Sharp rise in Pb (Fig. 2A)	88	79	97
Base-Pb	100	30	31	Airfall Pb onset (Fig. 2A)	125	108	147
HM15 ^{14}C age	220	37	41	^{14}C age (Garcés-Pastor *et al.* 2023)	83	74	92
Beta-301556	680	30	50	*Sphagnum* spp. remains	575	563	592
SUERC-43137	894	38	76	*Sphagnum* spp. remains	756	749	848
SUERC-43138	1069	38	103	*Sphagnum* spp. remains	1028	971	1054
Beta-326587	1290	30	116	*Sphagnum* spp. remains	1165	1099	1204
SUERC-43139	1394	35	133	*Sphagnum* spp. remains	1290	1208	1312
SUERC-43140	1483	36	158	*Sphagnum* spp. remains	1398	1363	1465
Beta-326588	1810	30	204	*Sphagnum* spp. remains	1721	1691	1763
SUERC-43141	1892	38	217	*Sphagnum* spp. remains	1819	1777	1866
SUERC-43142	2179	38	250	*Sphagnum* spp. remains	2123	2067	2162
Beta-301555	2210	30	266	*Sphagnum* spp. remains	2237	2182	2284
SUERC-43143	2420	38	320	*Sphagnum* spp. remains	2664	269	2692
SUERC-43146	2808	38	352	*Eriophorum vaginatum* and *Sphagnum*	2992	2923	3100
Beta-301557	3890	30	404	Bulk plant remains	4071	3709	4248

(following Daniels & Eddy 1990) and then expressed as proportions of the total *Sphagnum*.

Subfossil protozoa (testate amoebae) were extracted and identified following standard procedures (Ogden & Hedley 1980; Hendon & Charman 1997; Charman *et al.* 2000; Booth 2010; Amesbury *et al.* 2016) and quantified by counting at least 100 individual tests in each subsample (Payne & Mitchell 2009). Water table depth (WTD) reconstructions were obtained from the testate count percentages using a tolerance-downweighted weighted averaging model with inverse de-shrinking (WA-Tol inv) in the European transfer function of Amesbury *et al.* (2016) implemented in R (R Core Team 2020). Detrended correspondence analysis (DCA) (Fig. S2) was also applied to the testate amoebae data to characterize the most significant relationships between species and in the subfossil stratigraphy (Ter Braak & Prentice 1989; Ter Braak 1995; Woodland *et al.* 1998).

Physical properties and geochemistry

Major element and trace metal dry mass specific concentrations were determined using a Bruker S2 Ranger Energy-Dispersive X-ray fluorescence (ED-XRF): Si, Al, P, S, Ca, Mg, Cl, K, Fe, Mn, Ti (mg g^{-1}); As, Ba, Br, Cu, Ga, Pb, Ni, Nb, Rb, Sr, Y, Zn, Zr (μg g^{-1}). Freeze-dried subsamples at 10 mm intervals were hand ground, pressed and measured under a Helium atmosphere under combined Pd and Co excitation radiation and using a high resolution, low spectral interference silicon drift detector. The ED-XRF undergoes daily standardization procedures and has accuracies verified using 18 certified reference materials (e.g. Boyle *et al.* 2015; Schillereff *et al.* 2015). Total carbon (C) and total nitrogen (N) were measured using a Thermo Scientific Flash Smart Elemental Analyser. The C stratigraphy of peat sequences in ratio to N has also been used as an imperfect measure of peat decay with lower C:N if more decomposed (Malmer & Holm 1984; Kuhry & Vitt 1996; Biester *et al.* 2014). We calculated the ratio of total carbon to total nitrogen (C:N) as the molar ratio.

Peat humification, thermogravimetry, infrared and near-infrared spectrometry

The organic composition of the peat was characterized using a multi-method approach. The degree of peat humification, broadly the concentration of humic compounds, was measured using an alkali extraction procedure that digested 1 g of dried ground peat in 8% sodium hydroxide (NaOH). Percentage light transmission through a filtered (Whatman No. 1) extract was measured at 540 nm using the average of three repeats on a Jenway 6305 Ultraviolet/Visual spectrophotometer (Blackford & Chambers 1993). The organic content was analysed by pyrolysis (Yang *et al.* 2007), with differential scanning calorimetry (DSC) and thermogravimetry (TGA) recorded sequentially on a PerkinElmer STA6000 by heating samples 20 °C min^{-1} across the range 20–720 °C under a dynamic nitrogen air flow (10 L h^{-1}). Two high purity indium and silver standards (both 99.99%) were used to calibrate the STA6000 for both temperature (°C) and enthalpy (J g^{-1}) (Yang

et al. 2007). The TGA data were smoothed and expressed as mass loss 1st derivatives (mg).

FT-NIR spectra were measured on homogenized and hand-pressed dried samples at 10 mm contiguous intervals. All NIRS combined 24 scans collected at 40 cm^{-1} intervals across the range 3595–12 500 cm^{-1} on a Bruker MPA spectrometer. NIRS, focusing 8000–3800 cm^{-1} as containing the key organic spectral structure, were converted to 1st derivatives using a centrally weighted 9-point Savitzky–Golay smoothing algorithm minimizing noise. Data-transposed (depths as columns and wavenumbers rows) Principal Components Analysis (tPCA) using the Psych package (R Core Team 2020) was conducted using the NIR spectra for all samples in correlation mode and a varimax rotation (Martínez Cortizas *et al*. 2021, 2024). The NIRS were analysed further using multiple regression of 1st derivative spectra onto equivalent end members spectra measured for some known materials (Russell *et al*. 2019). Using end member materials appropriate for the composition of peat (Table S1) led to the derivation of regression coefficients that reflect the mixing proportions of the selected end members. The end member proportions are expressed as weight % once adjusted for the differing chromatic intensities of the selected end members (Russell *et al*. 2019). End member spectra multiple regression (EMS-MR) fitting (Russell *et al*. 2019) was conducted using the (LM) function in R (R Core Team 2020) in an iterative manner exploring the fits for combinations of three, four and five end member materials (Table S1). Reducing the end members to three (humin, Ericaceae and S*phagnum*) led to a significant improvement in the overall fit (R^2). The NIRS tPCA also identified three components (Cp1-3) accounting for ~99% of the overall variance. These better fits reflect the elimination of redundant signal from the spectral similarity of *Sphagnum* and *Eriophorum*, and humin and fulvic/humic acid standards (AvSHAFA). Ericaceae differentiates more strongly owing to the presence of lignin.

Attenuated total reflectance (ATR) FTIR spectra for the ground peat samples were obtained using a Bruker Alpha diamond crystal ATR spectrometer. FTIR were measured averaging 200 scans at 4 cm^{-1} resolution across the mid-infrared (MIR) region 4000–400 cm^{-1} (Martínez Cortizas *et al*. 2021, 2024). IR spectra were corrected using a 64-point flexible baseline in the Bruker OPUS software to negate bias in the signal due to scattering, reflection, temperature, concentration and instrument anomalies (e.g. Griffiths & De Haseth 1986) (Fig. S3). Data-transposed (wavenumbers as row and samples as columns) Principal Components Analysis (tPCA) was performed on baseline corrected ATR IR spectra to interrogate spectral patterns across all wavenumbers (Martínez Cortizas *et al*. 2021, 2024). The tPCA was conducted in correlation mode and used varimax rotation in the Psych package (R Core Team 2020). We have also calculated ratios between selected IR peaks (Fig. S3, Tables S2, S3) to determine the relative changes in functional groups or organic matter compounds (Martínez Cortizas *et al*. 2021).

Results

Geochronology, palaeoecology and palaeohydrology

The ^{14}C ages form a conformable sequence, alongside near surface airborne pollution markers dated independently within the region (Table 1, Fig. 2A). Those markers included atmospheric Pb (Le Roux *et al*. 2004; Goldsmith *et al*. 2013), Spheroidal Carbonaceous Particles (SCPs) (Rose & Appleby 2005; Garcés-Pastor *et al*. 2023) and mineral dusts (Ti and Zr) associated with 1960s motorway construction. All the age markers were included in a Bayesian age-depth model (Table 1) developed using 'rBacon' (Blaauw & Christen 2011) operating in the R environment (R-Core Team 2020). The Markov chain Monte Carlo repetitions were constrained by a gamma distribution with a 10-year cm^{-1} mean accumulation and shape 1.7 and a beta distribution with mean 0.26 and shape 25. These modelled chronologies (Fig. 2B) are used to constrain all down-core data.

The plant macrofossil, peat humification (Fig. 3) and testate amoebae stratigraphy (Fig. 4) characterizes the major changes in peatland development and has been subdivided into seven major zones (black lines on Figs 3, 4). Detailed pollen data are included in Fig. S1. The long-term development of the peatland commences with organic muds (zone I), a more eutrophic fen phase with abundant Monocotyledon remains including *Phragmites* (zone II), the establishment of oligo/ombrotrophic conditions with abundant Ericaceae remains (zone III) and the latter evolution of Holcroft Moss as a lowland ombrotrophic raised mire dominated by *Sphagnum imbricatum* (zones IV to VI). Through zones IV to VI, peaks in *Sphagnum* sect. *Acutifolia* and *Sphagnum tennelum* denote drier episodes, with *Sphagnum imbricatum* wetter conditions and *Sphagnum* sect. *Cuspidata* the wettest tolerance taxa. Zone VII contains the more recent developments when Holcroft Moss has been heavily affected by drainage, agriculture, peripheral commercial peat extraction and pollution (e.g. M62 motorway dust), where *Sphagnum* disappears, replaced by Monocotyledon remains mostly *Molinia caerulae*.

Structure in the testate amoebae stratigraphy at Holcroft Moss (Fig. 4) has been explored using detrended correspondence analysis implemented using PAST software (Hammer *et al*. 2001). Separation of species is good along both DCA axis 1 (eigenvalue = 0.5678) and axis 2 (eigenvalue = 0.2693) (Fig. S2) (Ter Braak 1995), with species arrangement along DCA axis 1 dominated by marked changes in community composition during the last 150 years. This period corresponds to anthropogenic drainage impacting on Holcroft Moss with abundant dry indicator taxa, for example, *Hyalosphenia subflava* and

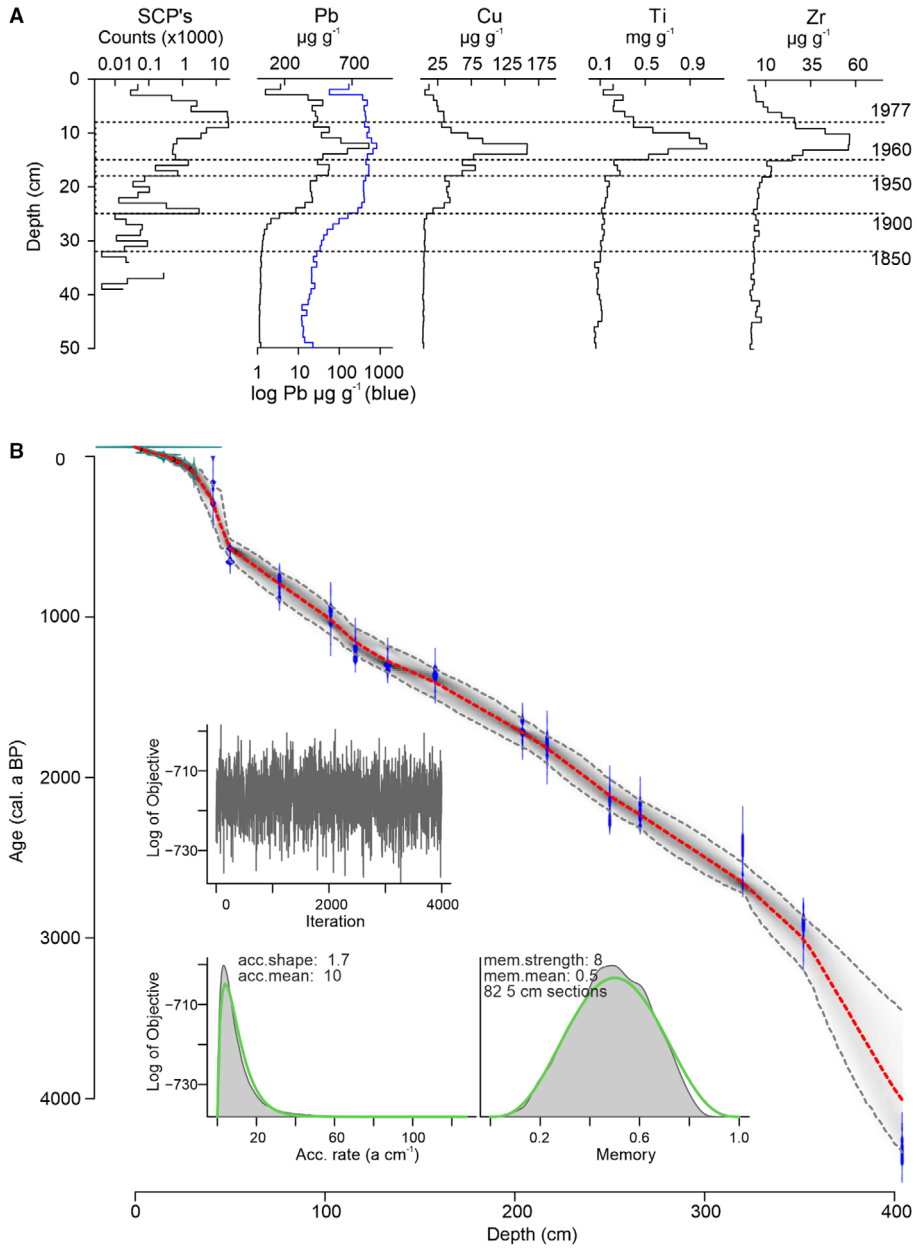

Fig. 2. A. Chronological markers airborne pollutants for Pb, Spheroidal Carbonaceous Particles (SCP), Pb, Cu and motorway dust markers (Ti, Zr µg g^{-1}). B. Age-depth model for Holcroft Moss using the pollution markers and 13 ^{14}C ages (blue) modelled using the Bayesian routine 'rBACON' in R (Blaauw & Christen 2011). The grey area represents the 95th confidence intervals, and the red line delineates the mean probability. Inset plots show 'fit' of all MCMC iterations of the run, the prior (green) and posterior (grey) distributions of accumulation rate (bottom left) and memory (bottom right) of the Bayesian model.

Cryptodifflugia oviformis-type. DCA axis 2 shows species distributed largely according to their tolerance of habitat wetness (Woodland *et al.* 1998; Charman *et al.* 2000; Amesbury *et al.* 2016), with dry indicator taxa, for example, *Hyalosphenia subflava* and *Trigonopyxis arcula*, at the opposite end to the wetter indicators, for example, *Archerella flavum* and *Amphitrema wrightianum*. The sample scores on DCA axis 2, therefore, form a semi-quantitative model summarizing fluctuations between wet (high values) and dry (low) conditions (Fig. 4). Reconstructions of depth to the water table (WTD) derived using a downweighted for tolerances weighted averaging model with inverse de-shrinking (WA-Tol inv) and the European transfer function (Amesbury *et al.* 2016) show a strong correlation (r = 0.553, $p = 3.64 \times 10^{-09}$) with DCA axis 2 (Fig. 4). Several species are only present and abundant in these surface layers, for example, *Nebela* and *Difflugia* species (Payne 2007;

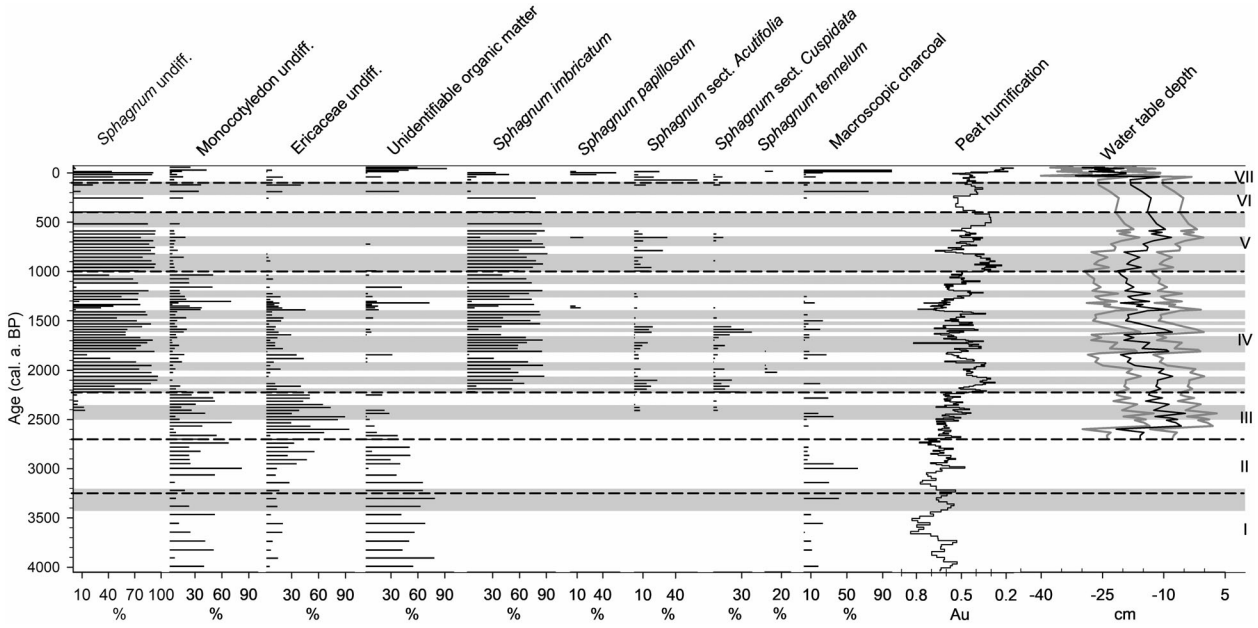

Fig. 3. Time series for plant macrofossil abundances (%), macroscopic charcoal, humification stratigraphy (light absorption units, axis reversed) and changes in peatland water tables (cm below the surface) reconstructed by ecological transfer function from testate amoebae data.

Mitchell *et al.* 2008), and they were excluded from WTD reconstructions (Swindles *et al.* 2019). There are strong down-core relationships between these semi-independent indicators of water table variations, and strong correspondence of wetter environment indicators denoting distinct wetter hydroclimatic episodes (shading on Figs 3, 4).

Organic components and decomposition dynamics

NIR spectra for Holcroft Moss (Fig. 5A) display broadly similar peaks and troughs throughout the core, with the average sample spectra sitting centrally to variations in amplitude. Data-transposed (depths as columns and wavenumbers rows) Principal Components

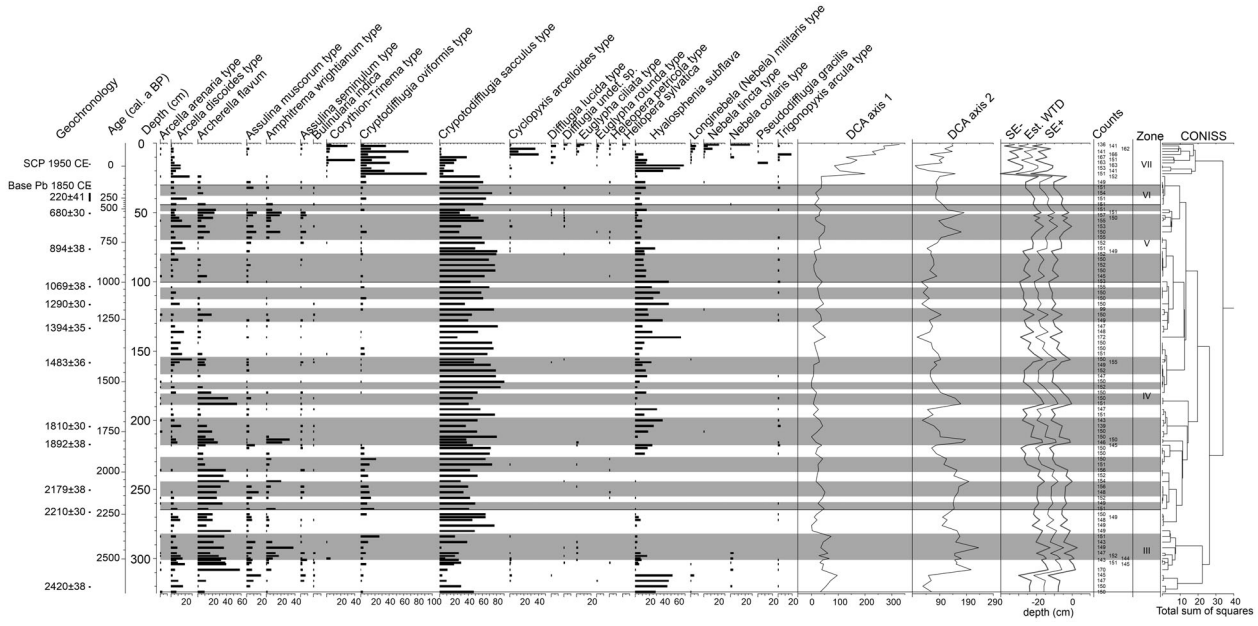

Fig. 4. Selected testate amoebae abundances plotted against age determinations, the age-depth model, and depth. Also shown are the sample scores for DCA axes 1 and 2, the reconstructed water table depths, and ± standard errors. The dendrogram shows a sum of squares cluster analysis implemented using CONISS (Grimm 1987). Pecked lines identify major peat stratigraphic boundaries, and shading denotes wetter phases in the development of Holcroft Moss.

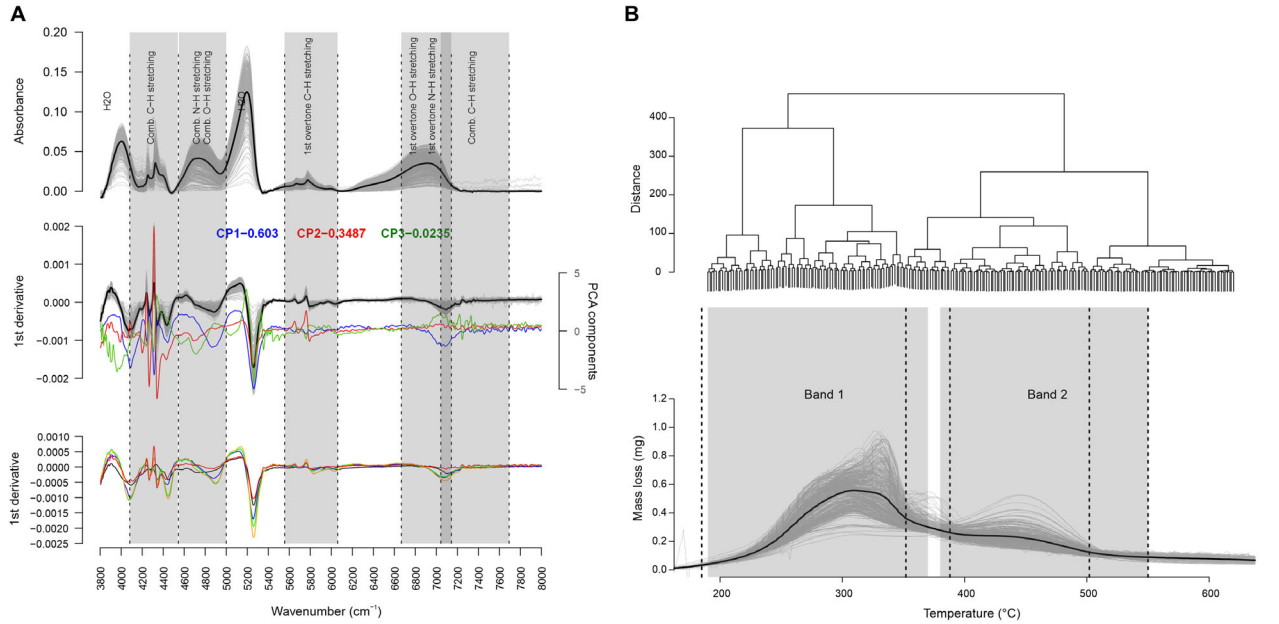

Fig. 5. A. Top: Cloud of the NIR spectra (top) baseline corrected absorbance spectra. Middle: first derivatives for all Holcroft Moss samples (Grey), the average 1st derivative (Black) and three PCA components (Cp1 to Cp3) spectra. Bottom: 1st derivative NIR spectra for selected end members (black = Average SHAFA; red = humin; blue = Sphagnum; green = Eriophorum; orange = Ericaceae; Table S1) in the Liverpool NIRS library. Grey shading denotes major organic and water NIRS bands (Stuart 2004). B. 1st derivative % mass loss spectra for the thermogravimetric data and cluster analysis dendrogram highlighting two major thermal windows for mass loss.

Analysis (tPCA) produced components 1 (Cp1) and 2 (Cp2), and they account for 60.3% and 34.9% of the variance in the data respectively (Fig. 5A). The NIR spectra for Cp1 and Cp2 are the inverse of each other in the regions 4545–4080 and 6060–5555 cm^{-1} relating to differences in abundance of combination C–H stretching and first overtone C–H stretching compounds (Stuart 2004). There are equivalent differences 5000–4545 and 7142–6666 cm^{-1} reflecting the combination N–H and O–H stretching along with first overtone N–H and O–H stretching regions (Stuart 2004). Broadly, these C-H compounds are abundant in Cp2 and lacking in Cp1, where both O-H and N-H stretching and first overtone peaks are stronger (Fig. 5A).

The end member spectra used here (Table S1) and the peat spectra show few differences, often sharing both peaks and spectral amplitude (Fig. 5A). The features in fresh plant matter spectra remain present but are heavily subdued in the humic/fulvic acid and humin end members. This spectral similarity is central to our doubt about whether alternative chemometric partial least squares regression methods for interrogating NIRS data could ever reconstruct the abundance of individual plant species (e.g. McTiernan *et al.* 1998).

The down-core patterns in tPCA Cp1-3 resemble strongly those reconstructed by End member spectra multiple regression (EMS-MR) for % humin, *Sphagnum*, and Ericaceae. The NIRS EMS-MR method thus appears successful at distinguishing between less and more decayed plant/peat components, with greater N–H compounds in the decayed materials. This accords with NIRS applications assessing animal fodder digestibility, where decay/digest of plant tissue dominates the spectral differences between fodder plants (Clark & Lamb 1991; Park *et al.* 1998; Givens & Deaville 1999; Decruyenaere *et al.* 2009). Ultimately, the EMS-MR of NIRS spectra generated down-core weight % data for three end members representing well-preserved cellulose-rich plants (*Sphagnum*) (Cp1), woody plant material (Ericaceae) (Cp3) and more decayed N-H organic materials (Humin) (Cp2).

The TGA data were smoothed and expressed as mass loss 1st derivatives (mg). Cluster analysis of the 1st derivative spectra identifies clear breaks in thermal behaviour at 150, 375–410 and 550 °C (Fig. 5B) defining major boundaries for quantifying the mass loss totals across 150–375 °C (Band 1) and 375–550 °C (Band 2). These bands match well-known ranges for thermal decomposition of (i) readily released compounds (e.g. sugars and cellulosic materials) from plant remains (150–375 °C) and (ii) more recalcitrant humic substances and lignin (375–550 °C) (Zaccone *et al.* 2018).

We used a multi-method approach to interpret the FTIR spectra for Holcroft Moss, given the challenges of interpreting the mid-infrared region for heterogeneous materials like peat (Coates 2000; Simonescu 2012; Martínez Cortizas *et al.* 2021, 2024). The FTIR spectra display distinctive regions of structure and wavenumber peaks that correspond with known organic constituents (Fig. S3, Tables S2, S3). The IR

spectral structure corresponds with greater relative differences in the organic matter composition shown as peaks in the standard deviation spectrum (Fig. S3). This between-sample variability is greatest at the IR peaks: 3340 (region I), 2980, 2920, 2850 (region II), 1710 (region IV), 1610 (region V), 1420, 1380 (region VI) and 1260, 1160 and 1030 cm^{-1} (region VII) (Fig. S3, Table S2).

Spectral Region I at Holcroft Moss comprises a broad absorption peak centred on 3340 cm^{-1} (3100–3600) typically related to hydroxyl (O–H) and N–H bond vibrations associated with cellulose and nitrogenated compounds. Region II comprises well-defined peaks at 2980, 2920 and 2850 cm^{-1} linked to C–H vibrations in aliphatic structures (Fig. S3, Table S2) from organic fats, wax, and lipids derived from peat forming plants (Chapman *et al.* 2001; Cocozza *et al.* 2003). Region III shows very low absorbances and little in the way of variation (standard deviation spectra, Fig. S3C), but the 2nd derivative spectra (Fig. 7D) reveal vibrations at 2160, 2050 and 1980 cm^{-1} related to the C≡N and C≡C bonds of aliphatic alkynes and nitriles (Stuart 2004). Region IV shows an IR peak at 1710 cm^{-1} and two second derivative peaks at 1733 and 1712 cm^{-1}, which can be related to polysaccharides (hemicellulose), but also to carboxylate and carboxylic groups formed by oxidation reactions (Chapman *et al.* 2001; Artz *et al.* 2008). Region V is dominated by the 1610 cm peak and smaller 1520 cm^{-1} peak, with 2nd derivative vibrations at 1608 and 1512 cm^{-1}. These vibrations most likely reflect aromatic compounds like lignin and other phenolic materials (Cocozza *et al.* 2003; Stuart 2004). Region VI contains the 1370 cm $peak^{-1}$ attributed to O–H and C–H deformations in phenolic and aliphatic groups (Cocozza *et al.* 2003; Artz *et al.* 2008). Region VII is dominated by the 1030 cm $peak^{-1}$ attributed to both C–O stretching and O–H deformation in polysaccharides (Cocozza *et al.* 2003). Other 2nd derivative peaks at 1260 and 1160 cm^{-1} are attributed to bond vibrations in syringyl/guaiacyl lignin structures (Cocozza *et al.* 2003; Martínez Cortizas *et al.* 2021). Region VIII is subdued in terms of IR absorbances, but 2nd derivative peaks at 897, 840 and 722 cm^{-1} have been associated with C–H out-of-plane vibrations in lignin and O–H stretching in polysaccharides (Artz *et al.* 2008; Martínez Cortizas *et al.* 2021).

The data-transposed Principal Components Analysis (tPCA) (Martínez Cortizas *et al.* 2024) reveals tPCA components 1 (Cp1) and 2 (Cp2) cumulatively account for 94.6% of the variance, hence strong matches of the Cp1 and Cp2 score spectra to the mean sample IR spectra (Fig. 6). The cellulose and polysaccharides 1030 and 3340 cm^{-1} peaks dominate Cp1 alongside opposed relationships to the aliphatic alkane and C–H stretching compound (2980, 2920 and 2850 cm^{-1}) peaks. Much of the Cp1 pattern is reversed on Cp2, which shows strong peaks 1260, 1610, 1710, 2850 and 2920 cm^{-1}—all typical of functional groups in lignin and organic acids, for example, aliphatic (i.e. alkanes, alkenes), car-

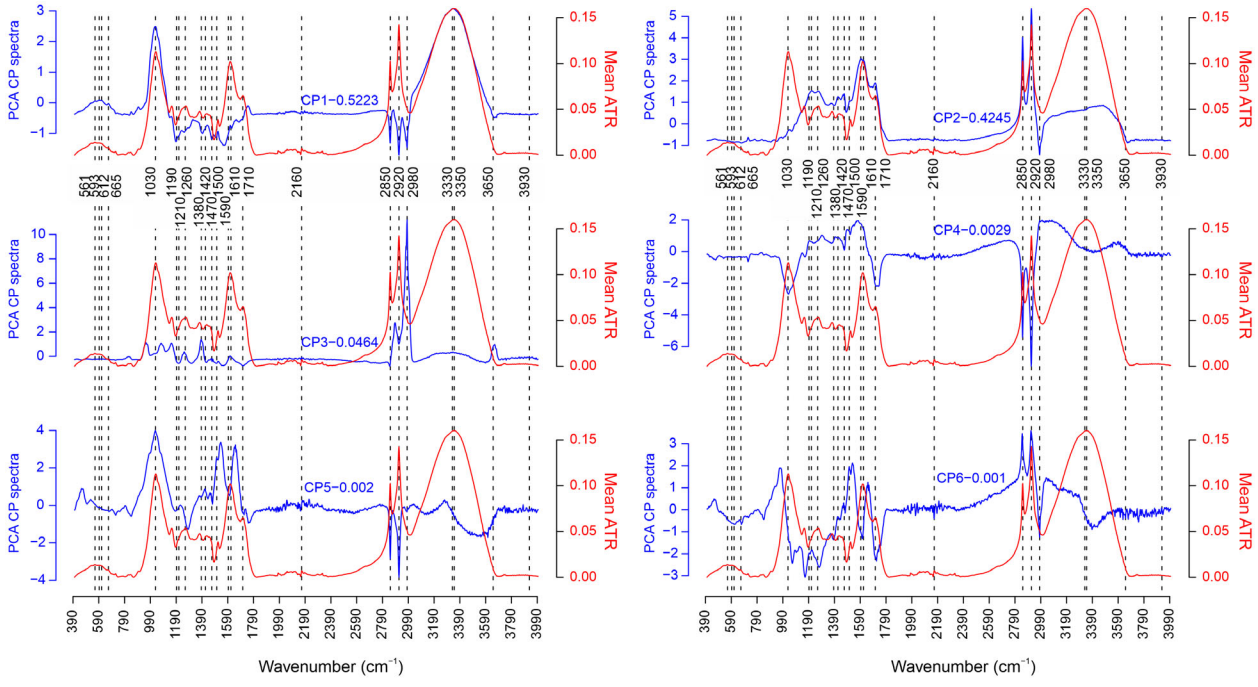

Fig. 6. Score spectra of components 1 to 6 (blue lines) of a varimax PCA conducted on transposed IR data matrix (Martínez Cortizas *et al.* 2024). The suffixes to the CP 1 to 6 labels reflect the percentage variation explained by each principal component as a fraction. For comparison, the red line shows the average IR spectrum of the Holcroft Moss samples. Annotations identify major FTIR spectral peaks (Table S3).

bonyl (i.e. acids, esters, aldehydes and ketones) and aromatic compounds (Martínez Cortizas *et al.* 2024). Down-core patterns in Cp1 and Cp2 are the inverse of each other, thereby documenting changes in abundance of labile (Cp1: cellulose and hemicellulose) versus recalcitrant (Cp2: lignin and aliphatic) organic compounds. IR1 and IR2 are ratios (Martínez Cortizas *et al.* 2021) that draw on some of those peaks (Table S3) and produce identical profiles that are the inverse of Cp1 and match Cp2 and quantify further this balance between labile and resistant organic matter.

Cp3 accounts for 4.6% of the variance, with a strong peak at 2980 cm^{-1} signifying aliphatic alkanes (methyl symmetric C–H stretching) (Stuart 2004), with further peaks at 2890, 1380 (aliphatic alkanes), 1253 (guaiacol lignin) (Rana *et al.* 2009), 1150 (C–O, cellulose, carbohydrates), 1070 and 955 cm^{-1} (carbohydrates/polysaccharides) (Stuart 2004; Martínez Cortizas *et al.* 2021, 2024). The ratio IR-3 ((2980 + 2920 + 2850)/1600 cm^{-1}) compares aliphaticity (CH_2, CH_3) versus aromaticity (Yao *et al.* 2012), and IR-8 (1265/1311 cm^{-1}) (G:S lignin ratio: Rana *et al.* 2009) both display similar down-core patterns to Cp3. Correspondence of these indicators with abundant Ericaceae macrofossils suggests the abundant lignin and aliphatic compounds are derived from woody ericaceous plants 2500–2000 cal. a BP. Earlier in the sequence, the declining IR-3 trend matches the wood-rich fen wetland phase 4000 to 2800 cal. a BP (Birks 1965, Fig. S1) preceding the major expansion of *Sphagnum* at Holcroft Moss *c.* 2250 cal. a BP.

The other tPCA components represent <0.7% of the total IR spectral variance and oscillate between strong positive and negative values. Cp4 shows positive loadings between 1700 and 1100 with several peaks offset slightly from the major organic components (Table S3), and negative loadings at 1030, 1710, 2850 and 2920 cm^{-1} (labile and recalcitrant organic components). Cp5 shows major positive loadings associated with aromatic compounds at 1620, 1520 (both C=C stretching) and 955 (C–H in-plane bending), and negative loadings at 2920, 2850 and 1260 cm^{-1} (aliphatic C–H stretching). These loadings reflect variations between high values for peat enriched in aromatic and low in aliphatic compounds, and low values for opposed conditions. Cp6 shows major positive loadings at 2915, 2850 (aliphatic CH stretching in fats, wax, lipids), 1560 (C=N aromatic skeletal vibrations) and a major peak at 980 cm^{-1} (polysaccharide C–O stretching). Strong negative loadings occur at 1515 (aromatic C=C stretching), and the 1200–-1050 cm^{-1} peak (aliphatic C–O or C–N stretching). In part, the Cp6 spectrum resembles that obtained previously for microbial biomass (Kamnev *et al.* 2021; Martínez Cortizas *et al.* 2024).

Nutrient concentrations and accumulation rates

Nutrient concentrations show quite different down-core profiles (Fig. 7). Carbon content is highest (55%) in the basal organic muds and fen peat phase (4000–2500 cal. a BP) and then decreases slowly and steadily over the last millennia (45%) before an abrupt dip (35%) near the bog surface. Nitrogen concentrations are also high (>1.5%) before 2500 cal. a BP and then fluctuate around 1.1%. N peaks (+>0.5%) are prominent in the C:N ratio around

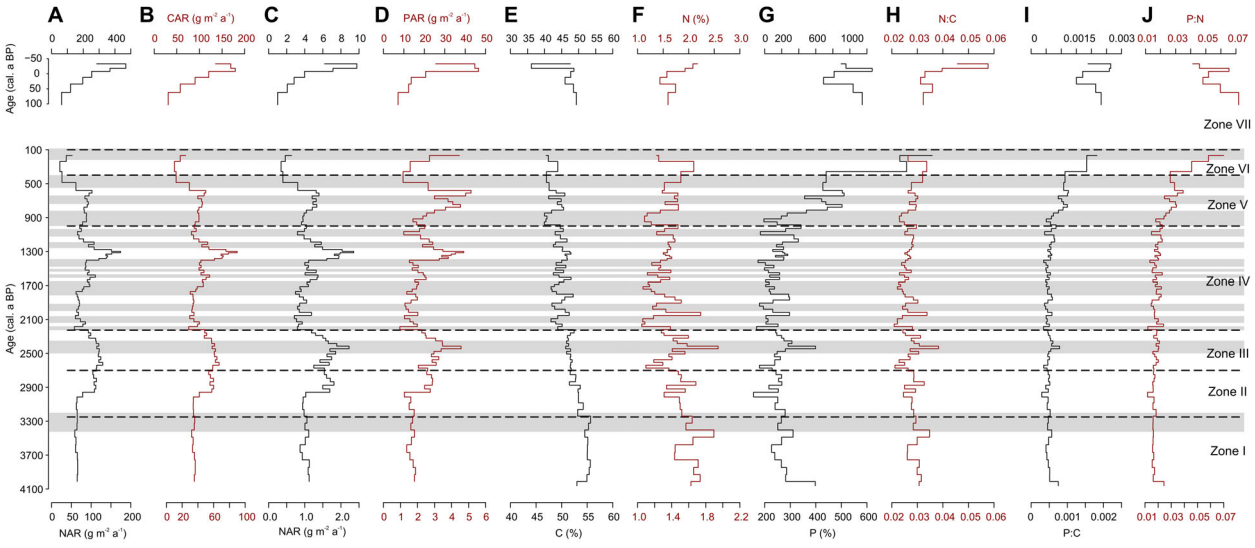

Fig. 7. Nutrient profiles for Holcroft Moss, plotting the surface peat separately to show elevated nutrient concentrations from cycling via living plant roots and materials. MAR represents total peat mass accumulation rate. CAR, NAR and PAR are the accumulation rates of carbon, nitrogen and phosphorus, respectively. Italicized numerals at the top of the left-hand plots denote maximum values, which have been cut off purely to maintain aesthetics. The N:C, P:C and P:N stoichiometric profiles are calculated and plotted inversely to much of the literature as changes in N and especially P drive fluctuations in the ratios. Pecked lines show the major peat stratigraphic zone boundaries, and shading denotes wetter phases taken from the testate amoebae and plant macrofossil analyses (Figs 3, 4).

2600–2200, 2000, 1800 and 500–200 cal. a BP. Through Zone IV to VI, troughs in C:N in part reflect the peat stratigraphy and can be attributed to wetter conditions. N concentrations rise to >2% in the last few centuries. Prior to 1000 cal. a BP, phosphorus shows modest fluctuations around a baseline of ~200 ppm, with low variability through the fen woodland and *Sphagnum*-dominated peat. P rises markedly from 1000 cal. a BP to the bog surface, with notable steps at 800, 400 cal. a BP and then peaking at ~1200 ppm in the surface layers. The P surface enrichment at Holcroft Moss resembles that of other UK and global peatlands and is the natural effect of phosphorus movement upwards via living plant roots and material (Schillereff *et al.* 2016). Whilst the maximum concentrations (1200–1300 ppm) are higher than other sites, the background levels (200 ppm) are spatially consistent, implying a national or latitudinal baseline. The rise in P from 1000 cal. a BP is associated stratigraphically and statistically with the behaviour of minerogenic and conservative elements, for example, Al (R = 0.82), Y (R = 0.6). K mirrors P, to some extent, but the increase begins slightly later within the last few centuries. A pronounced near-surface K spike coincides with Ca and probably reflects uptake by living *Sphagnum* fronds (Damman 1978) or on-site conservation grazing impacting the nutrient status for these uppermost samples.

The down-core P:C profile has two major phases, fluctuating modestly 4000–1000 cal. a BP and then increasing fourfold from 1000 cal. a BP. This equates to 100 cm depth, so proportional P enrichment cannot be a response purely to P recycling in the acrotelm (Damman 1978; Wang *et al.* 2015). Rather, this implies a shift in P behaviour that is independent of C and N dynamics over that timescale. Profiles for P:C, N:C and P:N demonstrate general synchronous fluctuations, but intervals of inverse behaviour appear at 1300–1200, 650–550 and 200–0 cal. a BP. Most shifts in decomposition are mirrored in the nutrient stoichiometry, with shading (Fig. 7) denoting P:N troughs and the intervening intervals capturing the P:N peaks.

Long-term (i.e. full-core) apparent accumulation rates of peat dry mass (MAR), C, N and P at Holcroft Moss are 91.5±3.4 dry peat g m^{-2} a^{-1}, 44.3±2.6 g C m^{-2} a^{-1}, 1.31±0.12 g N m^{-2} a^{-1} and 0.040±0.004 g P m^{-2} a^{-1}. These rates approach double that of the restricted set of other UK peatlands (Table 2) (Schillereff *et al.* 2016), which is a function of the lowland setting, proximity to agriculture and ~2000 years of more extensive forest disturbance recorded in pollen records from Holcroft Moss (Birks 1965; Fig. S1) and elsewhere in the northwest of England (Wells *et al.* 1997; Coombes *et al.* 2009; Fyfe *et al.* 2013). Other sites where C, N and P have been measured in parallel differ and are upland or expansive blanket peats. CAR and NAR are very tightly correlated throughout the core (R = 0.95). PAR also co-varies with C and N, including in the uppermost 40-cm (R > 0.75) and before 3000 cal. a BP, prior to establishment of *Sphagnum*. More rapid accumulation is observed at 3000–2200 and 1400–1200 cal. a BP, with the lowest rates during bog inception (pre-3000 cal. a BP), 2200–1400 a BP and in the striking deceleration between 500 and 200 cal. a BP.

Discussion

Stratigraphical relationships in the organic chemistry

Correlation coefficients and principal component analysis (Fig. 8) for the Holcroft Moss data suggest four groups of composition parameter down-core patterns. Group 1 parameters associate *Sphagnum*-rich poorly humified peat (high % light transmission) with low temperature pyrolysis components (TGA150–375 °C), and cellulose and polysaccharide IR signals (IR-Cp1, ratios IR1 and IR2). NIRS indicators for less decayed or fresher organic components form part of this group (NIR-Sphag and NIR-Cp1). The abundance of these components dominates the independent tPCAs conducted for the IR and NIR spectra, contributing 56% and 60% of the variance, respectively. Group 2 comprises more highly humified (absorbance) and carbon rich (% C) peat, alongside greater proportions of recalcitrant often unidentifiable (%UOM) organic materials, including high temperature pyrolysis materials (TGA375–550 °C) (Zaccone *et al.* 2018). High scores on IR-Cp2 reflect abundant recalcitrant lignin and aliphatic organic compounds. The IR3 and IR4 ratios plot

Table 2. Nutrient stoichiometric ratios in Holcroft Moss compared to other ombrotrophic bogs in the United Kingdom and across temperate latitudes outside the United Kingdom.

	C:N			C:P			N:P		
	Acrotelm[1]	Catotelm	Both	Acrotelm	Catotelm	Both	Acrotelm	Catotelm	Both
Holcroft Moss	29±1.97	37.3±0.4	36.5±0.5	535±35	1979±55	1836±66	18.9±1.2	52.8±1.2	49.4±1.5
UK peat[2]	31.7		41.2	1468		2160	45.4		50.9
Temperate peat[3]	37.5±3.8	45.8±3.7		1096±103	2654±514		29.7±2.4	54±6.8	

[1]Acrotelm/catotelm boundary treated as 40-cm unless reported otherwise.
[2]Schillereff *et al.* (2016).
[3]Schillereff *et al.* (2021).

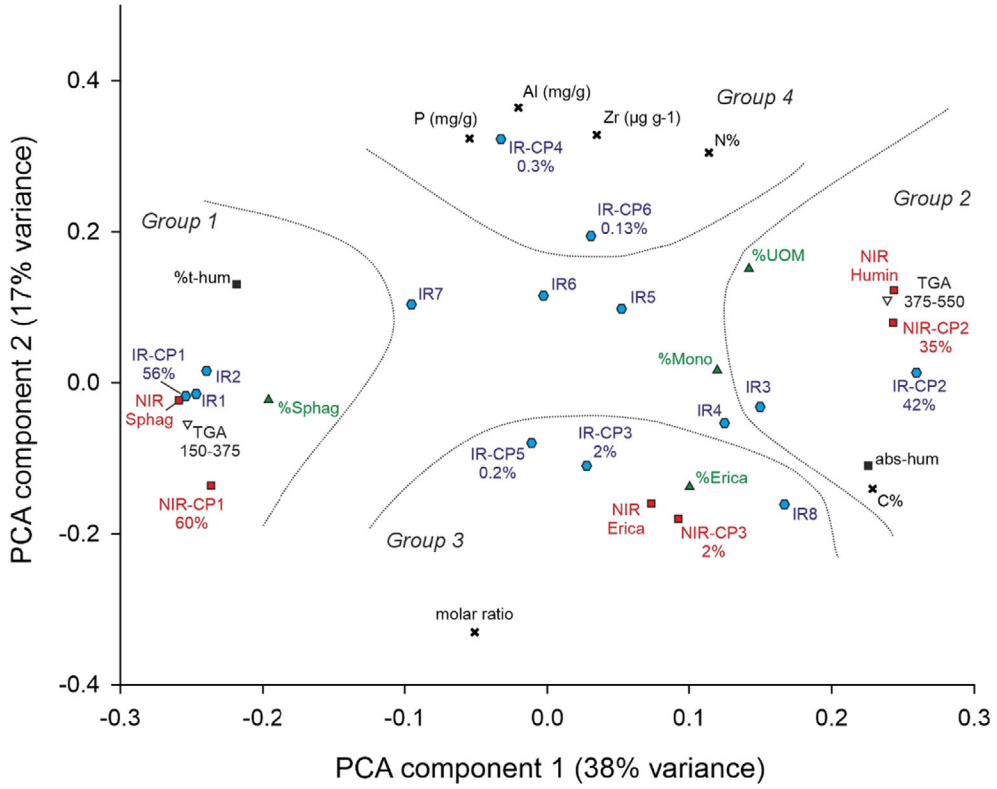

Fig. 8. Biplot of axes 1 and 2 of a principal component analysis of selected geochemical and organic composition parameters for the HM2012 core. Red (squares) denote NIRS parameters, FTIR (blue hexagons), TGA (black inverted triangles), plant macrofossils (green triangles), humification as % light transmission and absorption units (black squares) and geochemical parameters (black crosses).

close to Group 2 signifying more abundant aliphatic CH functional groups compared to aromatic. NIR indicators for more decayed C-H compounds are abundant in this group (NIR-Humin and NIR-CP2). These are the second most significant components of the IR and NIR spectra tPCAs contributing 42% and 35% of the variance respectively. Collectively, these Group 1 and 2 indicators correlate negatively, are widely separated on PCA component 1 and display inverse down-core patterns to each other (Figs 8, 9).

Group 3 comprises woody or lignin-rich proxy records containing abundant %Ericaceae, NIR-CP3, NIR-inferred Ericaceae alongside IR indicators of more abundant aromatic relative to aliphatic components (IR-CP3 and IR-CP5). Explaining ~2% or less of the total variance of tPCA for IR and NIR spectra, these components are abundant in restricted parts of the stratigraphy across zones II-III (3200 to 2225 cal. a BP) (Fig. 8), which developed as Holcroft Moss transitioned from a woody fen to ombrotrophic peatland (Birks 1965 and Fig. S1). Group 4 associates IR indicators of more abundant C=O carbonyls, N–H and C–N amides and aliphatic C–H alkenes (IR-CP4), alongside opposed enrichments in aliphatic, N-rich compounds (i.e. proteins) and polysaccharides (IR-CP6). IR-CP6 spectra also resemble that of microbial biomass (Kamnev *et al.* 2021). The proximity to %N suggests a link with the abundance of N-containing compounds. This group also displays a strong association with proxies for atmospheric dust deposition (Al and Zr) and elevated supply or retention of primary nutrients (P and N) (Fig. 8). The molar ratio C:N, often interpreted in relation to peat humification (Malmer & Holm 1984; Kuhry & Vitt 1996; Biester *et al.* 2014), displays no significant correlations with humification indicators (e.g. TGA150–375, average absorbance) only showing a strong negative correlation with % N ($r = -0.9474$, $p = 0.000$).

Peatland development and hydroclimate control of Holcroft Moss

The peat sequences of ombrotrophic raised mires have long been used in peatland development and palaeoclimate research (e.g. Blytt 1876; Weber 1903; Sernander 1908; von Post 1909; Granlund 1932). Given the ombrotrophic character of Holcroft Moss, many of the stratigraphical changes reflect the hydroclimate, with the peatland water table principally though not exclusively (Swindles *et al.* 2012) governed by summer moisture deficit: the balance between evapotranspiration water loss and precipitation gains (Charman *et al.* 2004, 2009; Booth 2010; Lehnhart-Barnett & Chiverrell 2025).

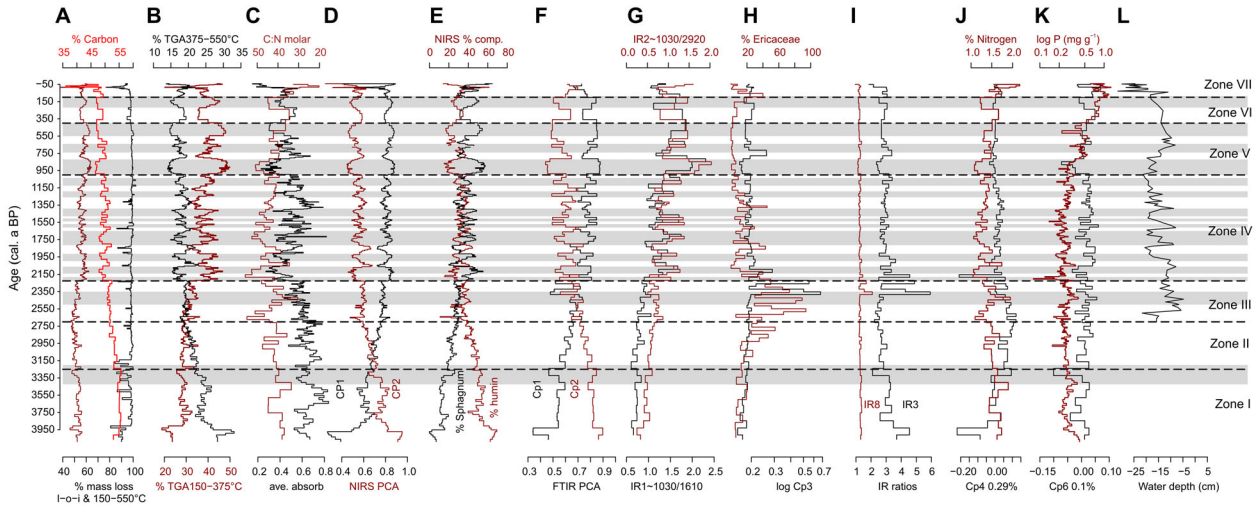

Fig. 9. Chronology of changes in the Holcroft Moss peat organic matter composition. A. Patterns in TGA thermal decomposition 150–550 °C (N atmosphere), loss-on-ignition (150–750 °C including air atmosphere) and total C%. B. TGA thermal decomposition 150–350 °C and 350–550 °C (N atmosphere). C. Peat humification (average absorption) and the C/N molar ratio. D. NIR tPCA components Cp1 and Cp2 showing opposed patterns in cellulose versus recalcitrant organic matter respectively. E. NIRS-inferred % Sphagnum (cellulose) and humin (recalcitrant humic substances and lignin). F. IR tPCA components Cp1 and Cp2 opposed summaries of abundant polysaccharides relative to aromatics or CH2 aliphatics. G. IR ratios denoting abundant polysaccharides relative to aromatics or CH_2 aliphatics. H. Macrofossil data on % Ericaceae remains and IR tPCA component Cp3 showing abundant lignin and aliphatic compounds. I. IR-3 aliphaticity (CH_2 and CH_3) versus aromaticity and the IR-8 guaiacol to syringol lignin ratio (Rana *et al.* 2009). J. IR tPCA component Cp4 summarizing N-containing compounds and total N%. K. Opposed enrichments in aliphatic N-rich compounds versus polysaccharides, and log total P (mg g^{-1}). L. Water table variations derived from the testate amoebae data. Pecked lines denote peat stratigraphy zone boundaries and shaded horizons are 'wetter' episodes with lower peat decomposition.

The establishment of Holcroft Moss occurred over underlying alluvial sands of the River Mersey terraces and is recorded in the basal peat (Zone I, 4050 to 3250 cal. a BP). These highly decomposed organic materials were dominated initially by monocotyledonous remains (*Phragmites australis*), containing abundant charcoal (Fig. 3) and large quantities of thermally mature aliphatic and aromatic organic compounds (Fig. 9). Cellulose and hemicellulose organic materials are not abundant throughout, but there are high and then declining FTIR signals for lignin and woody plant concentrations. Thus, Holcroft Moss established as a woody alluvial fen wetland *c.* 3200 cal. a BP.

In zone II the peat transitions to become increasingly poorly decomposed but remains dominated by aliphatic and aromatic organic matter (Fig. 9). From 2500 to 2250 cal. a BP (Zone III), the peat is dominated by woody Ericaceous remains with minor % monocotyledons and the first appearance of *Sphagnum* marking the probable onset of fully ombrotrophic conditions (Fig. 3). The FTIR data show indications of woody remains and lignin through zones I–III (4050 to 2225 cal. a BP). There is also a significant long-term trend in the state of decomposition illustrated well by FTIR tPCA Cp1 and Cp2 showing declines in aliphatic and aromatic organic matter relative to increases in poorly decomposed cellulose and polysaccharide compounds (Fig. 9F). These patterns are mirrored in the TGA mass loss 375–550 °C where the more recalcitrant humic substances and lignin gradually decline in abundance (Fig. 9B). Though predominantly well-humified throughout, these basal organic units (Zones I and II) show periods of less well-humified peat at *c.* 3500 and 3100 cal. a BP, which may be responses to wetter conditions (locally) or regional hydroclimate (Charman *et al.* 2006).

The expansion of *Sphagnum* to dominance 2250 cal. a BP (Zone IV) is the most substantial change in the stratigraphical record (Figs 3, S1) and is accompanied by a shift to poorly humified peat (low % light absorbance; Fig. 9C). The peat from 2250 to 250 cal. a BP subdivides into phases that reflect changing peatland surface wetness. Zone IV sees significantly different peat with greater concentrations of cellulosic and hemi-cellulosic organic matter, and overall, a less decomposed condition throughout (Fig. 9B–F). Lignin markers and Ericaceae macrofossils (Figs 3, 9H) decline in abundance through zone IV, punctuating a long-term trend towards reduced aliphatic and aromatic organic matter and greater cellulosic and hemi-cellulosic material (tPCA Cp1 and Cp2: Fig. 9F, G).

Zone IV is marked also by repeated fluctuations in composition, which are between units that contain fresher poorly decomposed materials (shaded bands, Fig. 9) dominated by *Sphagnum* remains, cellulose and hemicellulose organic matter. Conversely, the intervening more highly decomposed units of peat (unshaded, Fig. 9) are richer in recalcitrant aromatic and aliphatic compounds. Nine of the poorly decomposed units occur between 2225 and 1000 cal. a BP and are of differing

intensity and duration. The more well-humified peat contains abundant *Sphagnum* sect. *Acutifolia*, Ericaceae (Fig. 3), whereas the poorly humified peat comprises abundant *Sphagnum imbricatum* (c.f. *Sphagnum austinii*) or *Sphagnum papillosum*. Abundant *Sphagnum* sect. *Cuspidata* signifies the wettest of episodes 2250–2100, 1650–1550 and 720–600 cal. a BP. Macroscopic charcoal tends to peak in the drier episodes (Fig. 3). The more highly decomposed episodes are enriched with aliphatic (i.e. alkanes, alkenes), carbonyl (i.e. acids, esters, aldehydes and ketones) and aromatic compounds (often C-N and N-H) (Fig. 9). In zones V and VI, the switches between fresher poorly decomposed peat rich in cellulose and hemicellulose and more decomposed peat rich in aromatic and aliphatic components are greater in amplitude, more sustained and less frequent (Fig. 9). tPCA Cp6 summarizes opposed enrichments in aliphatic, N-rich compounds and polysaccharides and has been mooted as resembling microbial biomass IR spectra (Kamnev *et al*. 2021). tPCA Cp6 increases through zones V to VII paralleling the trends in P (mg g^{-1}) (Fig. 9K).

The most recent developments at Holcroft Moss (Zone VII) reflect denudation of the peat by drainage and conversion of surrounding lands to agriculture, intensive drainage and these concur with adjacent 20th century commercial peat extraction. The site is preserved as the only 'intact' uncut remnant (SSSI and NNR) of a formerly much more extensive lowland bog complex. Land-use changes associated with agriculture and construction of the M62 motorway have also substantially affected the airfall nutrient and pollutant flux to the peatland. Zone VII sees a substantial expansion of the drier indicating *Sphagnum* sect. *Acutifolia*, followed by *Sphagnum* disappearing entirely, with the peat comprising dominantly Ericaceae, monocotyledons (mostly *Molinia caerulea*) and decayed organic matter. There is also abundant macroscopic charcoal in these surface layers which corresponds to the period of peat extraction and drainage in the wider region impacting directly on Holcroft Moss and resulting in local fires. Zone VII displays sharp fluctuations in composition, but for the most part the peat is more highly decomposed, reduced in cellulose and hemicellulose markers and contains more abundant aromatic and aliphatic components (Figs 3, 9).

Our multi-proxy approach to characterizing the organic composition of Holcroft Moss shows significant changes in the decomposition of peat (Fig. 9B–G). Peat decomposition (or humification) can reflect changes in ecosystem surface wetness and hydroclimate. The minimum summer water table governs the duration of aerobic conditions experienced by peat whilst in the surface layers during accumulation (Clymo 1983, 1984a, 1991). The process of humification is typically limited to these aerobic conditions and so measures of down-core patterns of humic acid concentrations provide proxy records of changing peatland surface wetness (Bahnson 1968; Aaby & Tauber 1974; Blackford & Chambers 1991; Blackford & Chambers 1993). Hydroclimate interpretations of humification records are complicated by other factors influencing the signal, for example, differential decay rates between plant species (Yeloff & Mauquoy 2006; Zaccone *et al*. 2018). Broadly, the stratigraphy shows a long-term trend that correlates with age, with the peat increasingly decomposed and rich in recalcitrant organic compounds at greater depth. That trend is punctuated particularly in the last 2700 years by marked and repeated changes between Group 1 parameters showing poorly humified cellulose, polysaccharide and *Sphagnum*-rich peat and Group 2 dominated by more well-humified peat comprising more recalcitrant lignin and aliphatic organic compounds (Figs 8, 9). These changes in dominance are also interpreted as a response to shifts to wetter hydroclimate conditions mirroring equivalent signatures in the plant macrofossil and testate amoebae records (Figs 3, 4).

The Holcroft Moss plant macrofossil and testate amoebae stratigraphy (Figs 3, 4, 9L) shows shifts to wetter conditions centred *c*. 3450, 2600–2500, 2225, 2060, 2000, 1825, 1650–1610, 1540, 1480, 1260, 1125, 1000, 740–720, 600–550 and 220 cal. a BP. These wet shifts are quantified as water table fluctuations by testate amoebae record which also shows drier episodes 2750–2600, 2350–2250, 1920–1825, 1750–1650, 1200–790 cal. a BP culminating with the drying trend associated with disturbance of the bog in the surface peat from *c*. 220 cal. a BP. Most if not all the shifts to wetter conditions identified at Holcroft Moss feature in parallel investigations across northern Britain (Charman *et al*. 2006). These matches, within chronological uncertainties, include the substantial changes to wet conditions at 3450, 2600–2500 and 1650–1610 cal. a BP and the less substantial shifts at 2060, 1260, 740–720 and 600–550 cal. a BP. Correspondence of these wet shifts with those present at peatlands across the north of England and Europe confers some confidence as to the integrity and value of palaeoclimate records in peatlands (Charman *et al*. 2006, 2015; Swindles *et al*. 2012).

Nutrient co-regulation of peatland development

Locations where peat mass and C accumulation have been quantified in relation to nutrient load globally are few (n = 11: Schillereff *et al*. 2021); that database pointed to more atmospheric nutrient flux inhibiting carbon storage. Other peatland sites (Kylander *et al*. 2018; Ratcliffe *et al*. 2020) affected by more intense and event-scale nutrient input show conversely stimulation of carbon storage. The long-term carbon/nutrient accumulation rates at Holcroft Moss approach double those of other UK peatlands (Schillereff *et al*. 2019), but none of these sites are lowland ombrotrophic peatlands adjacent to intensive and persistent agricultural landscapes.

Thus, the Holcroft Moss record is the first developed for this type of peatland where persistent elevated levels of nutrient flux have stimulated greater carbon storage, highlighting divergent thresholds in the system response to changing nutrient loads for these important ecosystems. For the most part, the development of Holcroft Moss appears to be a story of hydroclimate variability driving shifts in vegetation, subfossil communities and decomposition of the peat, both as the peatland established (zones I–III) and through zones IV to V (Figs 3, 4, 9). There are patterns in the multi-proxy dataset for Holcroft Moss that, however, operate differently and require further explanation.

From Zone IV to Zone V, 2200 to 375 cal. a BP, there is a notable shift in the amplitude of the oscillations between more and less recalcitrant organic material, with Zone IV characterized by short-term fluctuations with a maximum period of a few decades (Fig. 10B). Zone V, on the other hand, after 1000 cal. a BP exhibits longer cycles of 200–100 years fluctuating between low and high decomposition. These patterns contrast with the combined or stacked Holocene peatland palaeowater table reconstructions from northern Britain (Charman *et al.* 2006), which match the pattern of more frequent oscillations in moisture conditions through the last 2000 years. One possibility is that this change in frequency is a response to changing nutrient dynamics. Phosphorus concentrations, and the P:N and P:C stoichiometric ratios, begin to rise from around 950 cal. a BP (Zone V). This coincides with greater input of airfall mineral material (e.g. Al, Zr; Fig. 10F), and predates the surface (0–15 cm) enrichment in P from the natural effects of phosphorus movement upwards via living plant roots and material. We postulate that contemporaneous landscape opening, inferred from the Holcroft Moss pollen record (Figs S1, 10H) and regional pollen-based landscape reconstructions (Fyfe *et al.* 2013), potentially destabilized surface soils, leading to greater local dust emission into the atmosphere and then redistribution of nutrients (Tipping *et al.* 2014). This soil flux would have brought P but less N, perhaps explaining the rising P:N ratio. Some P mineralization with Al or Fe oxides is likely (Damman 1978), but the sixfold increase in P concentrations across the top 1 m of peat almost certainly requires greater external input. Furthermore, in the PCA (Fig. 8) CAR and MAR plot close to the nutrients (both concentrations and ratios), perhaps evidencing that nutrient load is modulating the coupling of hydroclimate (bog wetness) and vegetation.

A series of peatland fertilization experiments show higher nutrient input can modify decomposition and carbon burial dynamics (Bubier *et al.* 2007; Fritz *et al.* 2012, 2014; Moore *et al.* 2019), although usually via the replacement of *Sphagnum* by shrub or herbaceous plants. At Holcroft Moss, zones V and VI are dominated by *Sphagnum imbricatum*, latterly replaced by *Sphagnum papillosum* in zone VII (Fig. 3). Through the period of *Sphagnum* dominance, *Sphagnum* section *Acutifolia* and *Sphagnum* section *Cuspidata* occasionally become more abundant during drier and wetter periods, respectively. Various drivers, including nutrient deposition,

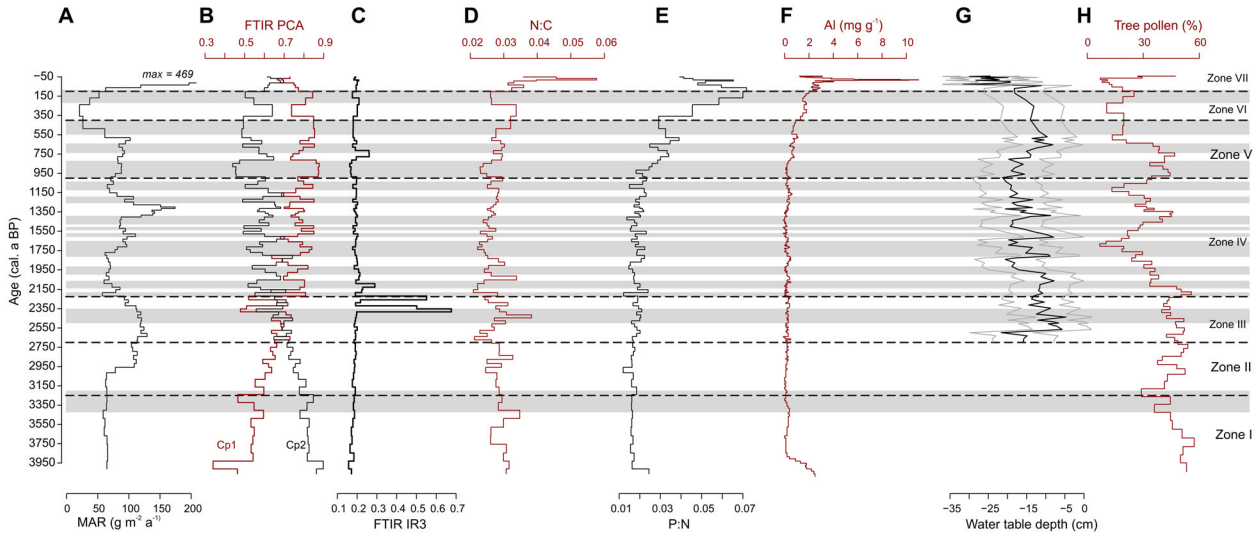

Fig. 10. Multi-proxy summary depicting key markers of variability in hydroclimate, vegetation, organic matter and nutrients over the 4000 years of bog development at Holcroft Moss. A. Peat mass accumulation rate. B–C. Organic constituents and their susceptibility to decomposition are captured by FTIR tPCA (Cp1 = sphagnum and Cp2 = humin) and FTIR IR3, which captures aliphaticity relative to aromaticity. D–F. Nutrient stoichiometry and mineral. N:C generally reflects a decomposition story of the proportional release of carbon relative to N. P:N illustrates strong P enrichment since 1000 cal. a BP as being independent of N. This coincides with a shift in amplitude of phases of more and less intense decomposition. The P curve follows Al concentrations, an indicator of allochthonous mineral dust deposition. G. Water table depths inferred from testate amoebae. H. Tree pollen proportion from the Holcroft Moss profile (Fig. S1) represents landscape openness in northwest England.

have been linked with the replacement of *Sphagnum imbricatum* (cf. *Sphagnum austinii*) by other *Sphagnum* species and other plants (Mauquoy & Barber 1999a; Robroek *et al*. 2007; Novak *et al*. 2008; McClymont *et al*. 2009; Swindles *et al*. 2015; McCarroll *et al*. 2016). However, *Sphagnum imbricatum* has responded strongly to elevated nutrient deposition through zones V and VI, only declining in zone VII with major anthropogenic drainage impacts, a greater frequency of surface fires (Slater & Slater 1978) and with the expansion of *Molinia caerulea* (Fig. 3). Intriguingly, manipulations as part of *Sphagnum* farming on rewetted bog grasslands (NW Germany) have also showed strong production of *Sphagnum* biomass, including oligotrophic species, under high nutrients (Vroom *et al*. 2020).

Major changes in peat mass accumulation, and, in turn, carbon and nutrients, often follow the hydroclimate-driven decomposition indicators, but there are periods where this co-behaviour breaks down. For instance, the striking acceleration in peat mass accumulation around 1350–1200 cal. a BP coincides with a wet shift, as expected, but earlier wet shifts did not trigger as much of an acceleration in peat mass accumulation (Fig. 10). These differences coincide with the increased presence of sedges during the 1350–1200 cal. a BP phase, whereas previous wet/dry transitions occurred within a *Sphagnum*-dominated setting. The early phases of bog development (Zones II and III) were dominated by various sedges (e.g. rapidly growing *Eriophorum* tussocks) and were also periods of high accumulation (Fig. 10), which then reduced as *Sphagnum* became established (Clymo 1984a). Taken together, this could be evidence that a departure from a particular vegetation—hydroclimate configuration pushes ecosystem functioning in such a way that the major plant species begin to change, bringing ecohydrological feedbacks that intensify or mute carbon accumulation (Swindles *et al*. 2012).

Zone VI displays the lowest dry peat and C mass accumulation rates (g m^{-2} a^{-1}) at Holcroft Moss (Fig. 10). This fall in rate begins in zone V *c*. 550 cal. a BP and coincides with a dramatic loss of *Sphagnum* replaced by greater proportions of unidentifiable organic matter, ericaceous shrub and monocotyledon plants (grasses and sedges). *Molinia caerulea* (purple moor grass) is currently abundant and has been dominant more recently across Holcroft Moss. *Molinia caerulea* has been identified as a problem species, lowering biodiversity and negatively impacting the condition status of peatlands as defined by national conservation agencies (e.g. Natural England). *Molinia*-covered peatlands carry a high risk of wildfire ignition (Marrs *et al*. 2004; Tomassen *et al*. 2004) and that is reflected in elevated macro and micro-charcoal concentrations in zones VI and VII. Some of the problems linked to *Molinia* domination are suppression of *Sphagnum* and other species impacting the provision of peatland ecosystem services. For example, reduced surface roughness lowers the natural flood protection function and reduces the peatland capacity to lock in carbon. Increased nutrient concentrations and fluxes (N, P, K) accompanied this shift from *Sphagnum* dominance, mimicking transitions as observed in fertilization experiments where nutrient deposition exceeds the capacity for processing by *Sphagnum* (Tomassen *et al*. 2004). This results in an excess of available P in the near-surface layers, allowing more nutrient demanding herbs and shrubs to take hold. Thus, human modification of the landscape through agricultural expansion, reduced woodland cover, and drainage activities have led to changes, sometimes positive and others negative, in peatland vegetation dynamics and, ultimately, carbon storage, from *c*. 950 to markedly after *c*. 500 cal. a BP (Fig. 10).

Conclusions

Parallel multi-proxy characterization of the organic matter composition and nutrient accumulation rates for Holcroft Moss shows a sequence dominated by switches between fresh, less decomposed layers and more decomposed peat containing abundant recalcitrant organic compounds. The stratigraphical record has been used to explore the interplay of rarely recorded nutrient and more widely used hydroclimate drivers for this lowland ombrotrophic peatland that is representative of many across northern Europe.

- Our multi-method (FTIR, FT-NIR and TGA) approaches characterizing the organic peat constituents at Holcroft Moss reveal a record of switches between fresher, poorly decomposed peat rich with cellulose and hemicellulose and more decomposed peat rich with aromatic and aliphatic compounds. These switches have dominated the last 3500 years of peatland development.
- Hydroclimate variability governs these decomposition patterns through much of the *Sphagnum*-dominated period at Holcroft Moss. These show responses to wetter conditions centred *c*. 3450, 2600–2500, 2225, 2060, 2000, 1825, 1650–1610, 1540, 1480, 1260, 1125, 1000, 740–720 and 600–550 cal. a BP. Wet episodes are punctuated by drier conditions 2750–2600, 2350–2250, 1920–1825, 1750–1650, 1200–790 cal. a BP, and a recent drying in the last 200 years trend associated with peatland disturbance.
- There are periods, however, where hydroclimate does not fully explain the variability observed and instead changes appear linked to the interplay between vegetation and nutrient dynamics. The amplitude of oscillations between more and less recalcitrant organic material changes from more rapid multi-decadal fluctuations 2200–1000 cal. a BP to longer cycles of 200–100 years after 1000 cal. a BP. This shift appears to be a response to changing nutrient dynamics with P

($\mu g\ g^{-1}$) and nutrient stoichiometric ratios (P:N and P:C) increasing from 950 cal. a BP, and that pattern is linked here to landscape opening and associated destabilized soils increasing the regional airborne nutrient flux. Elevated N and P deposition responding to various human activities at Holcroft Moss appear to have begun ~1000 cal. a BP, accelerated ~500 years cal. a BP.

- These carbon/nutrient accumulation rates at Holcroft Moss are high, and this first comprehensive nutrient stoichiometric record for a lowland UK ombrotrophic peatland shows that persistent elevated levels of nutrient flux have stimulated greater long-term carbon storage. This almost certainly is a function of adjacency to intensive and persistent agricultural landscapes and mimics the carbon accumulation responses to event scale nutrient influx seen at other peatlands globally (e.g. volcanic ash fall or dust storms).
- These stoichiometric relationships point to divergent trajectories and thresholds in the system response to changing nutrient loads for ombrotrophic peatlands, the largest terrestrial store of global carbon. Projections suggest elevated atmospheric nutrient loads will persist through the 21st century, and the implications of this for long-term bog resilience and carbon sink are unclear and will vary with the nature of peatland nutrient status and vegetation change. Differing trajectories of vegetation changes have occurred, associated with these increases in nutrient flux, for example, changes in *Sphagnum* species or complete *Sphagnum* decline. Peatland restoration and management projects typically focus on peatland hydrology and managing vegetation cover, but nutrient deposition rates need parallel consideration, and these require monitoring, assessment and management at a site scale.
- Vegetation, carbon and/or hydroclimate reconstructions exist for many temperate peatlands. Gaining a full understanding of the drivers of temperate bog development, therefore, depends on reconstructing in parallel changes in vegetation, hydroclimate, nutrients and organic constituents at high temporal resolution. A priority for future research should be to 'fill in the gaps' and reconstruct each missing node of the peatland carbon cycle, integrating surface wetness (or hydroclimate) reconstructions, concentrations of organic constituents and comprehensive assessment of the nutrient stoichiometry.

Acknowledgements. – For the purposes of Open Access, the authors have applied a Creative Commons Attribution (CC-BY) licence to any Author Accepted Manuscript version arising. We thank Jan A. Piotrowski, Joshua Ratcliffe and an anonymous reviewer for their insightful comments that have improved this manuscript. We thank Cheshire Wildlife Trust and Paul Thomas from Natural England for granting access permission to Holcroft Moss Site of Special Scientific Interest. The 2012 peat core was sampled, and the stratigraphical analyses (pollen, peat humification, testate amoebae and plant macrofossils) were undertaken by Julie Valentine (funded by a Liverpool John Moores University PhD Bursary). RCC and DNS were supported by Natural Environment Research Council (NERC) Research Grant NE/X010635/1. The radiocarbon measurements were funded by the Natural Environment Research Council through Radiocarbon Analysis Allocation Number 1619.0312. Fiona Russell's PhD (NIRS analyses) was supported by the School of Environmental Sciences, University of Liverpool. Josh Hicks (Central Teaching Laboratory, University of Liverpool) is thanked for running the FTIR measurements and Sabena Blackbird the total carbon and nitrogen analyses.

Author contributions. – Project leading: RC, DS and JK; funding acquisition: RC, DS, JK and DW; field investigations: RC, JK and JV; XRF geochemistry analyses: RC, JV, FR and JB; organic chemistry (Phosphorus, Nitrogen, Carbon): RC and DS; near-infrared spectrometry: FR, RC and JB; thermogravimetry: RC; Fourier transform infrared spectrometry: RC and DS; pollen, testate amoebae, plant macrofossil and peat humification analyses: JV, JK, DW; writing original draft: RC, DS and FR; comments and corrections: RC, DS and JK; figure and graphical production: RC, DS, FR and JV.

Data availability statement. – The data that support the findings of this study are available from the corresponding author upon reasonable request.

References

Aaby, B. & Tauber, H. 1974: Rates of peat formation in relation to degree of humification and local environment, as shown by studies of a raised bog in Denmark. *Boreas 4*, 1–17.

Aerts, R., Wallen, B. & Malmer, N. 1992: Growth-limiting nutrients in Sphagnum-dominated bogs subject to low and high atmospheric nitrogen supply. *Journal of Ecology 80*, 131–140. https://doi.org/10.2307/2261070.

Amesbury, M. J., Swindles, G. T., Bobrov, A., Charman, D. J., Holden, J., Lamentowicz, M., Mallon, G., Mazei, Y., Mitchell, E. A. D., Payne, R. J., Roland, T. P., Turner, T. E. & Warner, B. G. 2016: Development of a new pan-European testate amoeba transfer function for reconstructing peatland palaeohydrology. *Quaternary Science Reviews 152*, 132–151. https://doi.org/10.1016/j.quascirev.2016.09.024.

Artz, R. R. E., Chapman, S. J., Jean Robertson, A. H., Potts, J. M., Laggoun-Défarge, F., Gogo, S., Comont, L., Disnar, J. R. & Francez, A. J. 2008: FTIR spectroscopy can be used as a screening tool for organic matter quality in regenerating cutover peatlands. *Soil Biology and Biochemistry 40*, 515–527. https://doi.org/10.1016/j.soilbio.2007.09.019.

Bahnson, H. 1968: Kolorimetriske bestemmelser af humificeringstal i hojmosetørv fra Fuglsø Mose på Djursland. *Meddelelser Dansk Geologisk Forening 18*, 55–63.

Barber, K. E. & Charman, D. J. 2014: Holocene palaeoclimate records from peatlands. *In* Birks, J., Battarbee, R., Mackay, A. & Oldfield, F. (eds.): *Global Change in the Holocene*, 210–226. Routledge, London. https://doi.org/10.4324/9780203785027.

Barber, K. E. 1981: *Peat Stratigraphy and Climatic Change: A Palaeoecological Test of the Theory of Cyclic Peat Bog Regeneration*. 220 pp. Balkema, Rotterdam.

Biester, H., Knorr, K. H., Schellekens, J., Basler, A. & Hermanns, Y. M. 2014: Comparison of different methods to determine the degree of peat decomposition in peat bogs. *Biogeosciences 11*, 2691–2707. https://doi.org/10.5194/bg-11-2691-2014.

Birks, H. J. B. 1965: Pollen analytical investigations at Holcroft Moss, Lancashire and Lindow Moss, Cheshire. *Journal of Ecology 53*, 299–314. https://doi.org/10.2307/2257977.

Blaauw, M. & Christen, J. A. 2011: Flexible paleoclimate age-depth models using an autoregressive gamma process. *Bayesian Analysis 6*, 457–474. https://doi.org/10.1214/ba/1339616472.

Blackford, J. J. & Chambers, F. M. 1991: Proxy records of climate from blanket mires: evidence for a Dark Age (1400 BP) climatic deterioration in the British Isles. *The Holocene 1*, 63–67.

Blackford, J. J. & Chambers, F. M. 1993: Determining the degree of peat decomposition for peat-based palaeoclimatic studies. *International Peat Journal 5*, 7–24.

Blytt, A. 1876: *Essay on the Immigration of the Norwegian Flora During Alternating Rainy and Dry Periods*. 86 pp. A. Cammermeyer, Oslo.

Booth, R. K. 2010: Testing the climate sensitivity of peat-based paleoclimate reconstructions in mid-continental North America. *Quaternary Science Reviews 29*, 720–731. https://doi.org/10.1016/j.quascirev.2009.11.018.

Boyle, J. F., Chiverrell, R. C. & Schillereff, D. 2015: Approaches to water content correction and calibration for μXRF core scanning: comparing X-ray scattering with simple regression of elemental concentrations. *In* Croudace, I. W. & Rothwell, R. G. (eds.): *Micro-XRF Studies of Sediment Cores: Applications of a Non-destructive Tool for the Environmental Sciences*, 373–390. Springer, Dordrecht. https://doi.org/10.1007/978-94-017-9849-5_14.

Bubier, J. L., Moore, T. R. & Bledzki, L. A. 2007: Effects of nutrient addition on vegetation and carbon cycling in an ombrotrophic bog. *Global Change Biology 13*, 1168–1186. https://doi.org/10.1111/j.1365-2486.2007.01346.x.

Chambers, F. M., Beilman, D. W. & Yu, Z. 2011: Methods for determining peat humification and for quantifying peat bulk density, organic matter and carbon content for palaeostudies of climate and peatland carbon dynamics. *Mires and Peat 7*, 1–10.

Chapman, S. J., Campbell, C. D., Fraser, A. R. & Puri, G. 2001: FTIR spectroscopy of peat in and bordering scots pine woodland: relationship with chemical and biological properties. *Soil Biology and Biochemistry 33*, 1193–1200. https://doi.org/10.1016/S0038-0717(01)00023-2.

Charman, D. 2002: *Peatlands and Environmental Change*. 301 pp. Wiley, Chichester.

Charman, D. J. and 41 others 2013: Climate-related changes in peatland carbon accumulation during the last millennium. *Biogeosciences 10*, 929–944. https://doi.org/10.5194/bg-10-929-2013.

Charman, D. J., Amesbury, M. J., Hinchliffe, W., Hughes, P. D. M., Mallon, G., Blake, W. H., Daley, T. J., Gallego-Sala, A. V. & Mauquoy, D. 2015: Drivers of Holocene peatland carbon accumulation across a climate gradient in northeastern North America. *Quaternary Science Reviews 121*, 110–119. https://doi.org/10.1016/j.quascirev.2015.05.012.

Charman, D. J., Barber, K. E., Blaauw, M., Langdon, P. G., Mauquoy, D., Daley, T. J., Hughes, P. D. M. & Karofeld, E. 2009: Climate drivers for peatland palaeoclimate records. *Quaternary Science Reviews 28*, 1811–1819. https://doi.org/10.1016/j.quascirev.2009.05.013.

Charman, D. J., Blundell, A., Chiverrell, R. C., Hendon, D. & Langdon, P. G. 2006: Compilation of non-annually resolved Holocene proxy climate records: Stacked Holocene peatland palaeo-water table reconstructions from northern Britain. *Quaternary Science Reviews 25*, 336–350. https://doi.org/10.1016/j.quascirev.2005.05.005.

Charman, D. J., Brown, A. D., Hendon, D. & Karofeld, E. 2004: Testing the relationship between Holocene peatland palaeoclimate reconstructions and instrumental data at two European sites. *Quaternary Science Reviews 23*, 137–143. https://doi.org/10.1016/j.quascirev.2003.10.006.

Charman, D. J., Hendon, D. & Packman, S. 1999: Multiproxy surface wetness records from replicate cores on an ombrotrophic mire: implications for Holocene palaeoclimate records. *Journal of Quaternary Science 14*, 451–463. https://doi.org/10.1002/(SICI)1099-1417(199908)14:5<451::AID-JQS455>3.0.CO;2-N.

Charman, D. J., Hendon, D. & Woodland, W. A. 2000: *The identification of testate amoebae (Protozoa: Rhizopoda) in peats*. 147 pp. Quaternary Research Association, London.

Chiverrell, R. C. 2001: A proxy record of late Holocene climate change from May Moss, northeast England. *Journal of Quaternary Science 16*, 9–29. https://doi.org/10.1002/1099-1417(200101)16:1<9::AID-JQS568>3.0.CO;2-K.

Clark, D. H. & Lamb, R. C. 1991: Near infrared reflectance spectroscopy: a survey of wavelength selection to determine dry matter digestibility. *Journal of Dairy Science 74*, 2200–2205. https://doi.org/10.3168/jds.S0022-0302(91)78393-8.

Clymo, R. S. 1983: Peat. *In* Gore, A. J. P. (ed.): *Ecosystems of the World: Bog, Swamp, Moor and Fen*, 159–224. Elsevier, Amsterdam.

Clymo, R. S. 1984a: The limits to peat bog growth. *Philosophical Transactions of the Royal Society of London. B, Biological Sciences 303*, 605–654. https://doi.org/10.1098/rstb.1984.0002.

Clymo, R. S. 1984b: Sphagnum-dominated peat bog: a naturally acid ecosystem. *Philosophical Transactions of the Royal Society of London, Series B 305*, 487–499. https://doi.org/10.1098/rstb.1984.0072.

Clymo, R. S. 1991: Peat growth. *In* Shane, L. C. K. & Cushing, E. J. (eds.): *Quaternary Landscapes*, 76–112. Belhaven Press, London.

Coates, J. 2000: Interpretation of infrared spectra, a practical approach. *In* Meyers, R. A. (ed.): *Encyclopedia of Analytical Chemistry*, 10815–10837. Wiley, Chichester.

Cocozza, C., D'Orazio, V., Miano, T. M. & Shotyk, W. 2003: Characterization of solid and aqueous phases of a peat bog profile using molecular fluorescence spectroscopy, ESR and FT-IR, and comparison with physical properties. *Organic Geochemistry 34*, 49–60. https://doi.org/10.1016/S0146-6380(02)00208-5.

Coombes, P. M. V., Chiverrell, R. C. & Barber, K. E. 2009: A high-resolution pollen and geochemical analysis of late Holocene human impact and vegetation history in southern Cumbria, England. *Journal of Quaternary Science 24*, 224–236. https://doi.org/10.1002/jqs.1219.

Damman, A. W. H. 1978: Distribution and movement of elements in ombrotrophic peat bogs. *Oikos 30*, 480–495. https://doi.org/10.2307/3543344.

Daniels, R. E. & Eddy, A. 1990: *Handbook of European Sphagna*. 263. Institute of Terrestrial Ecology, Huntingdon.

Decruyenaere, V., Buldgen, A. & Stilmant, D. 2009: Factors affecting intake by grazing ruminants and related quantification methods: A review. *Biotechnology, Agronomy, Society and Environment 13*, 559–573.

Fletcher, W. & Ryan, P. 2018: Radiocarbon constraints on historical peat accumulation rates and atmospheric deposition of heavy metals at Holcroft Moss, Warrington. *North West Geography 18*, 18–28.

Fritz, C., Lamers, L. P. M., Riaz, M., Van Den Berg, L. J. L. & Elzenga, T. J. T. M. 2014: Sphagnum mosses – masters of efficient N-uptake while avoiding intoxication. *PLoS One 9*, e79991. https://doi.org/10.1371/journal.pone.0079991.

Fritz, C., van Dijk, G., Smolders, A. J. P., Pancotto, V. A., Elzenga, T. J. T. M., Roelofs, J. G. M. & Grootjans, A. P. 2012: Nutrient additions in pristine Patagonian Sphagnum bog vegetation: can phosphorus addition alleviate (the effects of) increased nitrogen loads. *Plant Biology 14*, 491–499. https://doi.org/10.1111/j.1438-8677.2011.00527.x.

Fyfe, R. M., Twiddle, C., Sugita, S., Gaillard, M.-J., Barratt, P., Caseldine, C. J., Dodson, J., Edwards, K. J., Farrell, M., Froyd, C., Grant, M. J., Huckerby, E., Innes, J. B., Shaw, H. & Waller, M. 2013: The Holocene vegetation cover of Britain and Ireland: overcoming problems of scale and discerning patterns of openness. *Quaternary Science Reviews 73*, 132–148. https://doi.org/10.1016/j.quascirev.2013.05.014.

Garcés-Pastor, S., Fletcher, W. J. & Ryan, P. A. 2023: Ecological impacts of the industrial revolution in a lowland raised peat bog near Manchester, NW England. *Ecology and Evolution 13*, e9807. https://doi.org/10.1002/ece3.9807.

Givens, D. I. & Deaville, E. R. 1999: The current and future role of near infrared reflectance spectroscopy in animal nutrition: a review. *Australian Journal of Agricultural Research 50*, 1131–1145. https://doi.org/10.1071/AR98014.

Goldsmith, B., Salgado, J. & Bennion, H. 2013: Using Novel Palaeolimnological techniques to define conservation objectives for hatch Mere. *ECRC research report 158*.

Gore, A. J. P. 1983: *Ecosystems of the World 4b Mires: Swamp, Bog, Fen and Moor – Regional Studies*. 480. Elsevier, Amsterdam.

Granlund, E. 1932: De svenska högmossarnas geologi. *Sveriges Geologiska Undersökning C 373*, 1–193.

Griffiths, P. R. & De Haseth, J. A. 1986: *Fourier Transform Infrared Spectrometry*. 535 pp. Wiley, Chichester.

Grimm, E. 1991: *TILIA and TILIAGRAPH*. Illinois State Museum, Springfield, IL.

Grimm, E. C. 1987: CONISS: a FORTRAN 77 program for stratigraphically constrained cluster analysis by the method of incremental sum of squares. *Computers and Geosciences 13*, 13–35. https://doi.org/10.1016/0098-3004(87)90022-7.

Hammer, Ø., Harper, D. A. T. & Ryan, P. D. 2001: Past: Paleontological statistics software package for education and data analysis. *Palaeontologia Electronica 4*, XIX–XX.

Hendon, D. & Charman, D. J. 1997: The preparation of testate amoebae (Protozoa: Rhizopoda) samples from peat. *Holocene 7*, 199–205. https://doi.org/10.1177/095968369700700207.

Holland, E. A., Dentener, F. J., Braswell, B. H. & Sulzman, J. M. 1999: Contemporary and pre-industrial global reactive nitrogen budgets. *Biogeochemistry 46*, 7–43. https://doi.org/10.1023/A:1006148011944.

Kamnev, A. A., Dyatlova, Y. A., Kenzhegulov, O. A., Vladimirova, A. A., Mamchenkova, P. V. & Tugarova, A. V. 2021: Fourier Transform Infrared (FTIR) spectroscopic analyses of microbiological samples and biogenic selenium nanoparticles of microbial origin: sample preparation effects. *Molecules 26*, 1146. https://doi.org/10.3390/molecules26041146.

Kilian, M. R., Van der Plicht, J. & Van Geel, B. 1995: Dating raised bogs: new aspects of AMS ^{14}C wiggle matching, a reservoir effect and climatic change. *Quaternary Science Reviews 14*, 959–966. https://doi.org/10.1016/0277-3791(95)00081-X.

Kuhry, P. & Vitt, D. H. 1996: Fossil carbon/nitrogen ratios as a measure of peat decomposition. *Ecology 77*, 271–275. https://doi.org/10.2307/2265676.

Kylander, M. E., Martínez-Cortizas, A., Bindler, R., Kaal, J., Sjöström, J. K., Hansson, S. V., Silva-Sánchez, N., Greenwood, S. L., Gallagher, K., Rydberg, J., Mörth, C. M. & Rauch, S. 2018: Mineral dust as a driver of carbon accumulation in northern latitudes. *Scientific Reports 8*, 6876. https://doi.org/10.1038/s41598-018-25162-9.

Le Roux, G., Weiss, D., Grattan, J., Givelet, N., Krachler, M., Cheburkin, A., Rausch, N., Kober, B. & Shotyk, W. 2004: Identifying the sources and timing of ancient and medieval atmospheric lead pollution in England using a peat profile from Lindow bog, Manchester. *Journal of Environmental Monitoring 6*, 502–510. https://doi.org/10.1039/b401500b.

Leah, M. D., Wells, C. E., Appleby, C. & Huckerby, E. 1997: *The Wetlands of Cheshire*. 246 pp. Lancaster University Archaeological Unit, Lancaster.

Legrand, M., McConnell, J. R., Bergametti, G., Plach, A., Desboeufs, K., Chellman, N., Preunkert, S. & Stohl, A. 2023: A two-fold increase of phosphorus in alpine ice over the twentieth century: contributions from dust, primary biogenic emissions, coal burning, and pig iron production. *Journal of Geophysical Research: Atmospheres 128*, e2023JD039236. https://doi.org/10.1029/2023JD039236.

Lehnhart-Barnett, H. T. & Chiverrell, R. C. 2025: Higher incidence of strongly evaporative days drives severe water deficit for ombrotrophic peatlands. *Hydrological Processes 39*, e70130. https://doi.org/10.1002/hyp.70130.

Limpens, J., Berendse, F. & Klees, H. 2004: How phosphorus availability affects the impact of nitrogen deposition on Sphagnum and vascular plants in bogs. *Ecosystems 7*, 793–804. https://doi.org/10.1007/s10021-004-0274-9.

Limpens, J., Heijmans, M. M. P. D. & Berendse, F. 2006: The nitrogen cycle in boreal peatlands. *In* Wieder, R. K. & Vitt, D. H. (eds.): *Boreal Peatland Ecosystems*, 195–230. *Ecological Studies 188*. Springer, Berlin.

Lin, X., Tfaily, M. M., Steinweg, J. M., Chanton, P., Esson, K., Yang, Z. K., Chanton, J. P., Cooper, W., Schadt, C. W. & Kostka, J. E. 2014: Microbial community stratification linked to utilization of carbohydrates and phosphorus limitation in a Boreal Peatland at Marcell Experimental Forest, Minnesota, USA. *Applied and Environmental Microbiology 80*, 3518–3530. https://doi.org/10.1128/AEM.00205-14.

Loisel, J. and 60 others 2014: A database and synthesis of northern peatland soil properties and Holocene carbon and nitrogen accumulation. *Holocene 24*, 1028–1042. https://doi.org/10.1177/0959683614538073.

Loisel, J., van Bellen, S., Pelletier, L., Talbot, J., Hugelius, G., Karran, D., Yu, Z., Nichols, J. & Holmquist, J. 2017: Insights and issues with estimating northern peatland carbon stocks and fluxes since the Last Glacial Maximum. *Earth-Science Reviews 165*, 59–80. https://doi.org/10.1016/j.earscirev.2016.12.001.

Magnan, G., van Bellen, S., Davies, L., Froese, D., Garneau, M., Mullan-Boudreau, G., Zaccone, C. & Shotyk, W. 2018: Impact of the Little Ice Age cooling and 20th century climate change on peatland vegetation dynamics in central and northern Alberta using a multi-proxy approach and high-resolution peat chronologies. *Quaternary Science Reviews 185*, 230–243. https://doi.org/10.1016/j.quascirev.2018.01.015.

Malmer, N. & Holm, E. 1984: Variation in the C/N-quotient of peat in relation to decomposition rate and age determination with ^{210}Pb. *Oikos 43*, 171–182. https://doi.org/10.2307/3544766.

Marrs, R. H., Phillips, J. D. P., Todd, P. A., Ghorbani, J. & Le Duc, M. G. 2004: Control of *Molinia caerulea* on upland moors. *Journal of Applied Ecology 41*, 398–411. https://doi.org/10.1111/j.0021-8901.2004.00901.x.

Martínez Cortizas, A., Sjöström, J. K., Ryberg, E. E., Kylander, M. E., Kaal, J., López-Costas, O., Álvarez Fernández, N. & Bindler, R. 2021: 9000 years of changes in peat organic matter composition in Store Mosse (Sweden) traced using FTIR-ATR. *Boreas 50*, 1161–1178. https://doi.org/10.1111/bor.12527.

Martínez Cortizas, A., Traoré, M., López-Costas, O., Sjöström, J. K. & Kylander, M. E. 2024: Beyond the obvious: exploring peat vibrational spectroscopy (FTIR-ATR) data using principal components analysis on transposed data matrix (tPCA), Store Mosse Bog (Sweden). *In* Núñez-Delgado, A. (ed.): *Frontier Studies in Soil Science*, 217–247. Springer International Publishing, Cham. https://doi.org/10.1007/978-3-031-50503-4_11.

Mauquoy, D. & Barber, K. 1999a: Evidence for climatic deteriorations associated with the decline of *Sphagnum imbricatum* Hornsch. ex Russ. in six ombrotrophic mires from northern England and the Scottish Borders. *Holocene 9*, 423–437. https://doi.org/10.1191/095968399673322360.

Mauquoy, D. & Barber, K. 1999b: A replicated 3000 yr proxy-climate record from Coom Rigg Moss and Felecia Moss, the border mires, northern England. *Journal of Quaternary Science 14*, 263–275. https://doi.org/10.1002/(SICI)1099-1417(199905)14:3<263::AID-JQS445>3.0.CO;2-W.

McCarroll, J., Chambers, F. M., Webb, J. C. & Thom, T. 2016: Informing innovative peatland conservation in light of palaeoecological evidence for the demise of sphagnum imbricatum: the case of Oxenhope Moor, Yorkshire, UK. *Mires and Peat 18*, 8. https://doi.org/10.19189/MaP.2015.OMB.206.

McClymont, E. L., Mauquoy, D., Yeloff, D., Broekens, P., van Geel, B., Charman, D. J., Pancost, R. D., Chambers, F. M. & Evershed, R. 2009: The disappearance of Sphagnum imbricatum from Butterburn Flow, UK: A reply to comments by Bjorn Robroek *et al*. *Holocene 19*, 1094–1097. https://doi.org/10.1177/0959683609345086.

McTiernan, K. B., Garnett, M. H., Mauquoy, D., Ineson, P. & Coûteaux, M. M. 1998: Use of near-infrared reflectance spectroscopy (NIRS) in palaeoecological studies of peat. *Holocene 8*, 729–740. https://doi.org/10.1191/095968398673885510.

Mitchell, E. A. D., Payne, R. J. & Lamentowicz, M. 2008: Potential implications of differential preservation of testate amoeba shells for paleoenvironmental reconstruction in peatlands. *Journal of Paleolimnology 40*, 603–618. https://doi.org/10.1007/s10933-007-9185-z.

Moore, P. D., Webb, J. A. & Collinson, M. E. 1991: *Pollen Analysis*. 216 pp. Blackwell, Oxford.

Moore, T. R., Knorr, K. H., Thompson, L., Roy, C. & Bubier, J. L. 2019: The effect of long-term fertilization on peat in an ombrotrophic bog. *Geoderma 343*, 176–186. https://doi.org/10.1016/j.geoderma.2019.02.034.

Novak, M., Erel, Y., Zemanova, L., Bottrell, S. H. & Adamova, M. 2008: A comparison of lead pollution record in Sphagnum peat with known historical Pb emission rates in the British Isles and the Czech Republic. *Atmospheric Environment 42*, 8997–9006. https://doi.org/10.1016/j.atmosenv.2008.09.031.

Ogden, C. G. & Hedley, R. H. 1980: *An Atlas of Freshwater Testate Amoebae*. 222 pp. Oxford University Press [for] the British Museum Natural History, Oxford.

Park, R. S., Agnew, R. E., Gordon, F. J. & Steen, R. W. J. 1998: The use of near infrared reflectance spectroscopy (NIRS) on undried samples of grass silage to predict chemical composition and digestibility parameters. *Animal Feed Science and Technology 72*, 155–167. https://doi.org/10.1016/S0377-8401(97)00175-2.

Payne, R. 2007: Laboratory experiments on testate amoebae preservation in peats: Implications for palaeoecology and future studies. *Acta Protozoologica 46*, 325–332.
Payne, R. J. & Mitchell, E. A. D. 2009: How many is enough? Determining optimal count totals for ecological and palaeoecological studies of testate amoebae. *Journal of Paleolimnology 42*, 483–495. https://doi.org/10.1007/s10933-008-9299-y.
R Core Team 2020: *R: A Language and Environment for Statistical Computing*. R Foundation for Statistical Computing, Vienna, Austria.
Rana, R., Langenfeld-Heyser, R., Finkeldey, R. & Polle, A. 2009: FTIR spectroscopy, chemical and histochemical characterisation of wood and lignin of five tropical timber wood species of the family of Dipterocarpaceae. *Wood Science and Technology 44*, 225–242. https://doi.org/10.1007/s00226-009-0281-2.
Ratcliffe, J. L., Lowe, D. J., Schipper, L. A., Gehrels, M. J., French, A. D. & Campbell, D. I. 2020: Rapid carbon accumulation in a peatland following Late Holocene tephra deposition, New Zealand. *Quaternary Science Reviews 246*, 106505. https://doi.org/10.1016/j.quascirev.2020.106505.
Robroek, B. J. M., Limpens, J., Breeuwer, A. & Schouten, M. G. C. 2007: Effects of water level and temperature on performance of four Sphagnum mosses. *Plant Ecology 190*, 97–107. https://doi.org/10.1007/s11258-006-9193-5.
Rose, N. L. & Appleby, P. G. 2005: Regional applications of lake sediment dating by spheroidal carbonaceous particle analysis I: United Kingdom. *Journal of Paleolimnology 34*, 349–361. https://doi.org/10.1007/s10933-005-4925-4.
Russell, F. E., Boyle, J. F. & Chiverrell, R. C. 2019: NIRS quantification of lake sediment composition by multiple regression using end-member spectra. *Journal of Paleolimnology 62*, 73–88. https://doi.org/10.1007/s10933-019-00076-2.
Schillereff, D. N., Boyle, J. F., Toberman, H., Adams, J. L., Bryant, C. L., Chiverrell, R. C., Helliwell, R. C., Keenan, P., Lilly, A. & Tipping, E. 2016: Long-term macronutrient stoichiometry of UK ombrotrophic peatlands. *Science of the Total Environment 572*, 1561–1572. https://doi.org/10.1016/j.scitotenv.2016.03.180.
Schillereff, D. N., Chiverrell, R. C., Croudace, I. W. & Boyle, J. F. 2015: An Inter-comparison of μXRF scanning analytical methods for lake sediments. *In* Croudace, I. W. & Rothwell, R. G. (eds.): *Micro-XRF studies of sediment cores: applications of a non-destructive tool for the environmental sciences*, 583–600. Springer, Dordrecht. https://doi.org/10.1007/978-94-017-9849-5_24.
Schillereff, D. N., Chiverrell, R. C., Macdonald, N., Hooke, J. M., Welsh, K. E., Piliposian, G. & Croudace, I. W. 2019: Convergent human and climate forcing of late-Holocene flooding in Northwest England. *Global and Planetary Change 182*, 102998. https://doi.org/10.1016/j.gloplacha.2019.102998.
Schillereff, D. N., Chiverrell, R. C., Sjöström, J. K., Kylander, M. E., Boyle, J. F., Davies, J. A. C., Toberman, H. & Tipping, E. 2021: Phosphorus supply affects long-term carbon accumulation in mid-latitude ombrotrophic peatlands. *Communications Earth & Environment 2*, 241. https://doi.org/10.1038/s43247-021-00316-2.
Sernander, R. 1908: On the evidences of postglacial changes of climate furnished by the peat-mosses of northern Europe. *GFF 30*, 465–473. https://doi.org/10.1080/11035890809445601.
Simonescu, C. M. 2012: Application of FTIR spectroscopy in environmental studies. *In* Farrukh, M. A. (ed.): *Advanced Aspects of Spectroscopy*, 49–84. InTechOpen, London. https://doi.org/10.5772/48331.
Slater, F. M. & Slater, E. J. 1978: The changing status of *Sphagnum imbricatum* Hornsch. ex Russ. on Borth Bog, Wales. *Journal of Bryology 10*, 155–161. https://doi.org/10.1179/jbr.1978.10.2.155.
Stuart, B. H. 2004: *Infrared Spectroscopy Fundamentals and Applications*. 224 pp. Wiley, Chichester.
Swindles, G. T. and 37 others 2019: Widespread drying of European peatlands in recent centuries. *Nature Geoscience 12*, 922–928. https://doi.org/10.1038/s41561-019-0462-z.
Swindles, G. T., Morris, P. J., Baird, A. J., Blaauw, M. & Plunkett, G. 2012: Ecohydrological feedbacks confound peat-based climate reconstructions. *Geophysical Research Letters 39*, L11401. https://doi.org/10.1029/2012GL051500.
Swindles, G. T., Turner, T. E., Roe, H. M., Hall, V. A. & Rea, H. A. 2015: Testing the cause of the *Sphagnum austinii* (Sull. ex Aust.) decline: multiproxy evidence from a raised bog in Northern Ireland. *Review of Palaeobotany and Palynology 213*, 17–26. https://doi.org/10.1016/j.revpalbo.2014.11.001.
Ter Braak, C. J. F. & Prentice, I. C. 1989: A theory of gradient analysis. *Advances in Ecological Research 19*, 1–55. https://doi.org/10.1016/S0065-2504(08)60183-X.
Ter Braak, C. J. F. 1995: Ordination. *In* Jongman, R. H. G., Ter Braak, C. J. F. & Van Tongeren, O. F. R. (eds.): *Data Analysis in Community and Landscape Ecology*, 91–173. Cambridge University Press, Cambridge.
Tipping, E., Benham, S., Boyle, J. F., Crow, P., Davies, J., Fischer, U., Guyatt, H., Helliwell, R., Jackson-Blake, L., Lawlor, A. J., Monteith, D. T., Rowe, E. C. & Toberman, H. 2014: Atmospheric deposition of phosphorus to land and freshwater. *Environmental Science: Processes & Impacts 16*, 1608–1617. https://doi.org/10.1039/c3em00641g.
Tipping, E., Davies, J. A. C., Henrys, P. A., Kirk, G. J. D., Lilly, A., Dragosits, U., Carnell, E. J., Dore, A. J., Sutton, M. A. & Tomlinson, S. J. 2017: Long-term increases in soil carbon due to ecosystem fertilization by atmospheric nitrogen deposition demonstrated by regional-scale modelling and observations. *Scientific Reports 7*, 1890. https://doi.org/10.1038/s41598-017-02002-w.
Toberman, H., Tipping, E., Boyle, J. F., Helliwell, R. C., Lilly, A. & Henrys, P. A. 2015: Dependence of ombrotrophic peat nitrogen on phosphorus and climate. *Biogeochemistry 125*, 11–20. https://doi.org/10.1007/s10533-015-0117-0.
Tomassen, H. B. M., Smolders, A. J. P., Limpens, J., Lamers, L. P. M. & Roelofs, J. G. M. 2004: Expansion of invasive species on ombrotrophic bogs: desiccation or high N deposition? *Journal of Applied Ecology 41*, 139–150. https://doi.org/10.1111/j.1365-2664.2004.00870.x.
Valentine, J., Davis, S. R., Kirby, J. R. & Wilkinson, D. M. 2013: The use of testate amoebae in monitoring peatland restoration management: case studies from North West England and Ireland. *Acta Protozoologica 52*, 129–145. https://doi.org/10.4467/16890027AP.13.0013.1110.
Vitousek, P. M., Aber, J. D., Howarth, R. W., Likens, G. E., Matson, P. A., Schindler, D. W., Schlesinger, W. H. & Tilman, D. G. 1997: Human alteration of the global nitrogen cycle: sources and consequences. *Ecological Applications 7*, 737–750. https://doi.org/10.1890/1051-0761(1997)007[0737:HAOTGN]2.0.CO;2.
von Post, L. 1909: Stratigraphische Studien über einige Torfmoore in Närke. *GFF 31*, 629–706. https://doi.org/10.1080/11035890909444807.
Vroom, R. J. E., Temmink, R. J. M., van Dijk, G., Joosten, H., Lamers, L. P. M., Smolders, A. J. P., Krebs, M., Gaudig, G. & Fritz, C. 2020: Nutrient dynamics of Sphagnum farming on rewetted bog grassland in NW Germany. *Science of the Total Environment 726*, 138470. https://doi.org/10.1016/j.scitotenv.2020.138470.
Wang, R., Balkanski, Y., Boucher, O., Ciais, P., Peñuelas, J. & Tao, S. 2015: Significant contribution of combustion-related emissions to the atmospheric phosphorus budget. *Nature Geoscience 8*, 48–54. https://doi.org/10.1038/ngeo2324.
Weber, C. A. 1903: Über Torf, Humus und Moor. Versuch einer Begriffsbestimmung mit Rücksicht auf die Kartiertrog und die Statistik der Moore. *Abhandlungen Des Naturwissenschaftlichen Vereins Zu Bremen 17*, 465–484.
Wells, C., Huckerby, E. & Hall, V. 1997: Mid- and late-Holocene vegetation history and tephra studies at Fenton Cottage, Lancashire, U.K. *Vegetation History and Archaeobotany 6*, 153–166. https://doi.org/10.1007/BF01372568.
Wilkinson, D. M. 2023: *The Fundamental Processes in Ecology: Life and the Earth System*. 176. Oxford University Press, Oxford.
Woodland, W. A., Charman, D. J. & Sims, P. C. 1998: Quantitative estimates of water tables and soil moisture in Holocene peatlands from testate amoebae. *Holocene 8*, 261–273. https://doi.org/10.1191/095968398667004497.
Yang, H., Yan, R., Chen, H., Lee, D. H. & Zheng, C. 2007: Characteristics of hemicellulose, cellulose and lignin pyrolysis. *Fuel 86*, 1781–1788. https://doi.org/10.1016/j.fuel.2006.12.013.
Yang, Q., Liu, Z. & Bai, E. 2023: Comparison of carbon and nitrogen accumulation rate between bog and fen phases in a pristine peatland

with the fen-bog transition. *Global Change Biology 29*, 6350–6366. https://doi.org/10.1111/gcb.16915.
Yao, S., Cao, J., Zhang, K., Jiao, K., Ding, H. & Hu, W. 2012: Artificial bacterial degradation and hydrous pyrolysis of suberin: implications for hydrocarbon generation of suberinite. *Organic Geochemistry 47*, 22–33. https://doi.org/10.1016/j.orggeochem.2012.03.005.
Yeloff, D. & Mauquoy, D. 2006: The influence of vegetation composition on peat humification: implications for palaeoclimatic studies. *Boreas 35*, 662–673.
Yu, Z., Loisel, J., Brosseau, D. P., Beilman, D. W. & Hunt, S. J. 2010: Global peatland dynamics since the Last Glacial Maximum. *Geophysical Research Letters 37*, L13402. https://doi.org/10.1029/2010GL043584.
Zaccone, C., Plaza, C., Ciavatta, C., Miano, T. M. & Shotyk, W. 2018: Advances in the determination of humification degree in peat since Achard (1786): Applications in geochemical and paleoenvironmental studies. *Earth-Science Reviews 185*, 163–178. https://doi.org/10.1016/j.earscirev.2018.05.017.

Supporting Information

Additional Supporting Information to this article is available at http://www.boreas.dk.

Fig. S1. Percentage pollen data for the 2012 Holcroft Moss peat profile with pollen and spore counts expressed as percentages of total land pollen. These data provide the % tree pollen data on Fig. 9. The dendrogram shows a sum of squares cluster analysis implemented using CONISS (Grimm 1987). Pecked lines identify zones in the vegetation history.

Fig. S2. Biplot of axes 1 and 2 of detrended correspondence analysis for testate amoebae species, using abbreviations of the names from Fig. 4.

Fig. S3. Raw ATR-FTIR spectra, baseline corrected ATR-FTIR spectra each overlayed with the mean spectra, the standard deviation spectrum and second derivative spectrum for the Holcroft Moss samples. Annotations identify major FTIR regions (I to VIII), spectral peaks and 2nd derivative vibrations (Table S2).

Table S1. End member materials used in the NIRS end member multiple regression (Russell *et al*. 2019).

Table S2. IR bands identified at Holcroft Moss and published assignment of the peaks to organic components ([1] Chapman *et al*. 2001; [3] Cocozza *et al*. 2003; [4] Artz *et al*. 2008; [2] Heller *et al*. 2015; [6] Martínez Cortizas *et al*. 2021, 2024).

Table S3. IR peak ratios used, and their basis (Martínez Cortizas *et al*. 2021, 2024).